Manuscript

Journal of Energy Engineering, Volume 146, Issue 4, 2020, Article number 04020023
DOI: 10.1061/(ASCE)EY.1943-7897.0000673

Integrated Simulation Framework for Assessing Turbocharger Fault Effects on Diesel Engine Performance and Operability

Konstantinos Ntonas [1]; Nikolaos Aretakis [2]; Ioannis Roumeliotis [3] ;
Efthimios Pariotis[4] ; Yiannis Paraskevopoulos[5] and Theodoros Zannis[6]

Abstract: Turbocharged diesel engines are extensively used in marine vessels, both as propulsion engines and as generator sets. The engines operation in the hostile marine environment results to performance degradation having a negative effect on the economics of the marine vessel's operation both in terms of fuel consumption and maintenance. This paper presents a turbocharged 4-stroke diesel engine simulation framework based on one-dimensional calculations and analysis. The framework is suitable for turbomachinery and heat exchanger components fault simulation predicting both turbocharger and diesel engine performance and operability. Meanline models were used in conjunction with beta lines method for generating accurate and detailed compressor and turbine performance maps, coupled with a single zone closed-cycle diesel engine model for generating engine performance characteristics. The simulation framework modules are adjusted and validated against measured data. Following specific faults are simulated utilizing physical consistent parameters such as blade friction and thickness based on relevant literature data. Overall system simulation and operation analysis is carried out assessing operability and performance parameters. Analysis results show a significant reduction in engine performance, especially in case of both turbo-components being fouled (22% power reduction), in contrast with the heat exchanger fouling where the power reduction is about 1%.

Author keywords: Turbocharger; Diesel Engine; Centrifugal Compressor; Radial Turbine; Turbocharger fault effects;

[1]Research Assistant, Laboratory of Thermal Turbomachines, School of Mechanical Engineering, National Technical University of Athens. Email: kntonas@central.ntua.gr (corresponding author)

Published by American Society of Civil Engineers. This is the Author Accepted Manuscript issued with: Creative Commons Attribution Non-Commercial License (CC:BY:NC 4.0). The final published version (version of record) is available online at DOI:10.1061/(ASCE)EY.1943-7897.0000673. Please refer to any applicable publisher terms of use.

[2]Assistant Professor, Laboratory of Thermal Turbomachines, School of Mechanical Engineering, National Technical University of Athens. Email: naret@central.ntua.gr

[3]Assistant Professor, Section of Naval Architecture & Marine Engineering, Hellenic Naval Academy, Piraeus Greece, also Lecturer at Cranfield University. Email: I.Roumeliotis@cranfield.ac.uk

[4]Assistant Professor, Section of Naval Architecture & Marine Engineering, Hellenic Naval Academy. Email: pariotis@snd.edu.gr

[5] Founder-Technical Director of Turbomed SA Email: turbomed@otenet.gr

[6] Assistant Professor, Section of Naval Architecture & Marine Engineering, Hellenic Naval Academy. Email: thzannis@snd.edu.gr

Notation

AL0	=	Compressor diffuser outlet angle, Turbine nozzle inlet angle.	Q_{comb}	=	In-cylinder fuel combustion energy input
AL1	=	Compressor diffuser inlet angle, Turbine nozzle outlet angle.	$Q_{comb,tot}$	=	Total heat of combustion
ALR3	=	Compressor impeller exit sweep angle, Turbine impeller inlet angle	Q_W	=	Heat transfer through the boundaries of the engine cylinder
B4	=	Compressor impeller inlet angle, Turbine impeller exit angle	R	=	Resistance
CC	=	Centrifugal Compressor	R0	=	Compressor diffuser outlet radius, Turbine nozzle inlet radius
C.P, C.T	=	Charged Air Pressure and Temperature	R1	=	Compressor diffuser inlet radius, Turbine nozzle outlet radius
$C_{piston,mean}$	=	Mean piston speed	R3	=	Compressor impeller outlet radius, Turbine impeller inlet radius
dP	=	Pressure Drop	R4	=	Compressor impeller inlet radius, Turbine impeller outlet radius
HDDI	=	Heavy-Duty Direct Injection	Re	=	Reynolds number
HS0	=	Compressor diffuser height at outlet radius, Turbine nozzle height at inlet radius	RH	=	Relative Humidity
LHV	=	Lower Heating Value of Diesel fuel	RT	=	Radial Turbine
m_{AIR}	=	Diesel engine inlet air mass flow rate	Sfc	=	Specific fuel consumption
m_{cor}		Corrected mass flow ($\dot{m}\sqrt{\theta}/\delta$)	T4,T5	=	Temperature before and after Radial Turbine
m_{EXH}	=	Diesel engine exhaust gas mass flow rate	RBDW	=	Compressor impeller outlet width, Turbine impeller inlet width
m_{fuel}	=	Diesel engine fuel mass flow rate	T/C	=	Turbocharger

N	=	Diesel engine crankshaft speed, T/C speed	T_{cyl}	=	In-cylinder Temperature
n	=	Polytropic exponent	TH1	=	Compressor diffuser leading edge normal thickness, Turbine nozzle trailing edge normal thickness
N_c	=	T/C Corrected speed ($N/\sqrt{\theta}$)	TH4	=	Compressor impeller inlet normal thickness, Turbine impeller exit normal thickness
$N_{c,des}$	=	T/C Design corrected speed	T_{exh}	=	Exhaust gas temperature
NRBL	=	Number of impeller full blades	T_{IVC}		Cylinder gas temperature at inlet valve closing
NRSBL	=	Number of impeller splitter blades	T_{EVO}	=	Cylinder gas temperature at exhaust valve opening
NSTV	=	Number of stator vanes	T_{im}	=	Temperature at diesel engine inlet manifold
η_{vol}	=	Diesel engine volumetric efficiency	U	=	Overall Heat Transfer Coefficient
P_{amb}	=	Ambient Pressure	U_{cyl}	=	Internal Energy of the engine cylinder content
p_{cyl}	=	In-cylinder pressure	V_{SW}	=	Diesel engine Cylinder swept volume
P_{EVO}	=	Cylinder gas pressure at exhaust valve opening	W	=	Engine work output
$P_{exh,manif}$	=	Gas pressure at exhaust manifold	$\Delta\varphi_c$	=	Duration of combustion (in CA degs)
P_{im}	=	Pressure at diesel engine inlet manifold	ε	=	Effectiveness
Pr	=	Prandlt number			

Introduction

Turbocharged diesel engines have been widely used in vehicles, heavy duty trucks, ships, non-interconnected electric power systems and other energy applications. Specifically, they have a leading role in marine industry, used mainly as main propulsion engines and as auxiliary power generator sets (GENSETs). Naval vessels up to frigate class utilize four-stroke diesel engines for propulsion as well as GENSETs since they offer lower acquisition cost, better fuel economy and better response to load changes compared to gas turbines (Bricknell, 2006).

As discussed by Button et al. (2015), the bigger contributors in the life cycle cost of the turbocharged diesel engines are maintenance and operational costs. The development of an integrated simulation framework for simulating fault effects on turbocharged diesel engines is expected to contribute towards

quantifying the degradation effect on operational cost by providing information on the increased fuel consumption and decreased load (Murphy et al., 2015). At the same time, it may provide information on maintenance cost and operability concerning compressor surge margin reduction along with temperature and rotational speed changes that affect bearings life. Additionally, it can be used for providing suitable fault signatures, as discussed by Pagán Rubio et al. (2018).

Turbocharger (T/C) consists of two components, a Centrifugal Compressor (CC) and a Radial (RT) or Axial Turbine depending on diesel engine size. The impact of turbocharger modeling on diesel engine combustion mechanism and performance characteristics have been thoroughly examined in the past by Giakoumis and Tziolas (2018) and by Giakoumis et al. (2017). Also the influence of turbocharger heat transfer modeling both for diesel and gasolines engine performance parameters have been investigated using neural networks by Huang et al. (2018). At present, the design and modeling of both T/C components can be performed by using 1D and 3D analysis. 1D analysis is used to calculate components performance maps using basic geometrical parameters and not the whole geometry in contrast to 3D analysis. Thus, it can be a powerful tool during preliminary design and modeling. In 1D analysis the flow through the impeller is assumed uniform and the off-design performance is calculated using mean streamline single zone models (Galvas 1973, Aungier 1995, Wasserbauer and Glassman 1975). A significant aspect for the compressor map is the prediction of surge line. Rodgers (1963) set the surge and choke limits for a wide range of centrifugal compressors using experimental data. Another approach was made by Japikse (1996), who assumed that a jet-wake structure exists in the impeller passage. Stuart et al. (2017) made a new approach in CC 1D analysis using a three-zone model assuming that impeller exit recirculation influences compressor work input. For the turbine performance, 1D models have been extensively applied, as for example described by Romagnoli and Martinez–Botas (2011) utilizing mean line analysis method well described in the past (e.g. Wasserbauer and Glassman 1975). Applying 1D models for T/C component faults simulation and map prediction allows for assessing the fault effect using physical consistent parameters such as roughness increase rather than arbitrary mass flow and efficiency reduction factors used in the literature (Pagán Rubio et al. 2018) providing information, at the same time, of the fault effect on the surge line.

Studies conducted in the past have examined the effect of various faulty conditions on marine diesel engine performance characteristics. Specifically, Kökkülünk et al. (2016) investigated the performance degradation of a marine diesel engine by using curve-based approach and Kowalski (2015) developed a methodology of a multidimensional diagnostic tool based on exhaust gas composition of marine engines. Also, Sakellaridis et al. (2015) proposed a turbocharger simulation methodology for marine two-stroke diesel engine modeling and diagnostic applications.

The 3D model provides a high-fidelity analysis, based on CFD simulation and as a time, consuming method, it is used in most cases, as a designing and stability analysis tool. It is also combined with 1D model, for loss correlations adaptation. Japikse and Baines (1997) suggested a turbomachinery component design procedure, combining 1D and 3D model, a procedure followed by Qiu et al (2013), in T/C components design.

The importance of the turbomachinery component maps used as part of a turbocharged engine model has been highlighted by Pesiridis et al. (2012). As discussed, suitable fitting and extrapolation methods should be applied for accurately predicting the engine performance.

In the present work the well-established beta lines method suggested by Kurzke (1996) is applied for ensuring accurate interpolation and extrapolation both for compressor and turbine performance maps generated by corresponding meanline models, described in next section. Various types of models have been proposed and used in the literature for the simulation of performance and emissions of turbocharged diesel engines, depending on the application and configuration examined (Watson and Janota, 1982). Three are the main categories of diesel engine models: zero-dimensional thermodynamic models, quasi-dimensional phenomenological models and multi-dimensional CFD models. In zero-dimensional thermodynamic models (Baldi et al. 2015 and Catania et al. 2011) the heat release is simulated in a simplified way, using empirical / mathematical expressions, without detailed study of physical and chemical sub-processes that actually take place in the combustion chamber, because these are strongly dependent on the spatial distribution of temperature and composition which are not taken into account. This approach is advantageous in applications where limited data are available regarding the design configuration and the operating parameters of the engine, while computational power is limited, and

102 computational time is a critical parameter. In the field of phenomenological simulation models, quite
103 important are the multi-zone combustion models, which provide a temporal and spatial distribution of
104 combustion temperature and mixture composition based on the concept of fuel jet distribution into zones.
105 A fair compromise between more detailed multi-zone and single-zone combustion models is provided by
106 two-zone combustion models, which offer reasonable accuracy at economic computer runtime
107 (Rakopoulos et al., 2003). Two-zone models have been used very effectively for examining the effect of
108 exhaust gas recirculation (EGR) rate and temperature on diesel engine combustion characteristics and
109 pollutant emissions as demonstrated by Rakopoulos et al. (2018). Phenomenological models along with
110 experimental campaigns have been used by Rakopoulos et al. (2015) and Rakopoulos et al. (2019) to
111 examine the effect of various alternative fuels on HDDI turbocharged diesel engine performance
112 characteristics and pollutant emissions under both steady-state and transient conditions.

113 On the other hand, the multidimensional CFD models (Petranović et al. 2018, Reitz and Rutland 1995
114 and Liang et al. 2010) are based on locally resolved solution of conservation of mass, energy and
115 momentum and include detailed sub-models for spray and combustion phenomena. With this approach it
116 is possible to obtain detailed results regarding the gas flow pattern and the spatial distribution of
117 temperature and composition inside the combustion chamber. However, these models are very demanding
118 in terms of detailed design data, computational power and expertise to be applied making its use
119 appropriate only for specific applications.

120 The intermediate category is the quasi-dimensional phenomenological models, which allows to
121 execute efficient, fast and economic preliminary calculations of heat release models and exhaust
122 emissions as a function of important engine parameters like injection pressure, injection timing, swirl
123 ratio and boost pressure. These models are based on physical and chemical sub-models for fuel spray
124 formation, air fuel mixing, combustion and emission formation, offering a fair compromise between the
125 detailed CFD ones and the zero-dimensional models, being appropriate as predictive tools conducting
126 parametric studies during engine development (Pagán Rubio et al. 2018, Pariotis and Hountalas 2003 and
127 2004, Pariotis et al. 2005).

Focusing on models applied to investigate the matching between diesel engine and a turbocharger system, Charlton (1992) proposed the SPICE modeling software, which is a quasi-dimensional model, based on the filling and emptying method and is particularly suited for turbocharged diesel engine systems. The system of components is modeled as a combination of thermodynamic volumes, flow junctions and shafts. The intake and exhaust valves are represented by junctions, each having a schedule of effective flow area versus crankshaft position. One dimensional compressible flow equations are used to obtain flow rates for given pressures in the neighboring volumes. The performance of the turbocharger compressor and turbine is represented by tabulated data taken from performance maps published by the manufacturers.

An alternative approach has been proposed by Ledger et al. (1971 and 1973), focusing on the transient simulation of turbocharged engines, by linking steady speed experimental data (regarding engine performance and gas flow) with dynamic models of the mechanical components of the system. However, the weakness of this approach is that it is heavily dependent on experimental data and it oversimplifies the simulation of combustion. A more comprehensive transient model (extended from the filling and emptying model) was developed by Watson and Marzouk (1977). Their model was used to investigate turbocharger response problems at a fundamental level. It takes into account the non-linear influence of combustion on the torque developed and the exhaust-gas energy available at the turbine, the pulsating nature of gas flow (including reverse flow) and also the influence of manifold pressure on pumping work.

The increasing need for marine engine system downsizing, combined with the harsh working conditions, leads to frequent engine components failure, especially for the turbocharger. In order to ensure ship safety operation, by preventing those failures, a fault diagnosis system must be used. For turbocharger fault diagnosis, slight improvement has been made, comparing with the rest of turbomachines (e.g. turbofan, gas turbine, etc.), relying in most cases on engineers' personal experience. At present, Barelli et al. (2009) presented a turbocharger diagnosis methodology based on Artificial Neural Network (ANN) and proposed a frequent data gathering campaign every 6 to 9 months in order to ensure the proper operation of such a system. Sakellaridis and Hountalas (2013) also developed a radial turbine mean line code for being a part in a T/C diagnostic tool with the ability of adapting to available

155 measured data. Cui et al. (2018) developed a gas-path diagnosis for diesel engine turbochargers, using
156 health factors (flow capacity and isentropic efficiency), hence monitoring the T/C health status.

157 The present study proposes a turbocharged diesel engine modeling framework using 1D modeling for
158 T/C components, single zone modeling for the diesel engine and matching analysis between T/C and
159 diesel engine. The diesel engine model is adapted to engine specific data and the overall integrated model
160 is validated against shop trials data obtained from a marine diesel generator. Having developed a model
161 capable to simulate the system operation over its whole envelope, engine fouling analysis is performed in
162 order to determine how fouling in T/C and intercooler affects the whole system operation**.**

163 The T/C component faults simulation is materialized using physical consistent parameters such as
164 roughness increase rather than arbitrary mass flow and efficiency reduction factors (Kurz and Brun 2009)
165 or time consuming CFD analysis (Melino et al. 2011) used in the literature. In this way the fault effect on
166 the surge line is provided, thus the effect of faults on operability, usually neglected in the literature, is
167 assessed as well.

168 ## Integrated Simulation Platform

169 The integrated simulation platform utilizes 1D models for calculating the T/C component maps based
170 on the available geometry, then a fully coupled process integrating the T/C components the diesel engine
171 and the intercooler is applied for calculating the performance and operating conditions at sub-system and
172 system level.

173 ### Turbocharger Modeling

174 The turbocharger can be modeled by using specific compressor and turbine maps, a feature that can
175 be applied when measured maps are available or when the geometry of the turbocharger is not available.
176 In the latter case appropriate scaled maps can be used. In the case that measured turbomachinery
177 geometry is available or the simulation system is used as part of an integrated pre-design or/and
178 optimization procedure, or specific faults are to be simulated, suitable mean line aerothermodynamic
179 models are used for calculating the component maps. A hybrid modeling approach can also be applied, for
180 example using a measured map for the compressor and a map calculated based on geometry for the
181 turbine.

For simulating Variable Geometry, either in the case of Inlet Guide Vanes for the compressor and Variable Guide Vanes for the turbine the simulation tool can handle multimaps performing 3-D interpolations as discussed by Alexiou et al. (2012). If the meanline codes are applied for the T/C components modeling then the Variable Geometry is integrated to the calculations, since the maps are derived for specific inlet angles allowing the optimization of the Variable Turbine control schedule as part of a design process, or the simulation of variable geometry fault for assessing its effect on operability and performance.

Centrifugal Compressor

For calculating the compressor map, namely the relation between corrected mass flow rate, pressure ratio and efficiency for different corrected rotational speeds an in-house compressor meanline code is used. The 1-D code is based on the methodology presented in (Galvas, 1973). The flow properties are calculated along a streamline in mean radial position using Wiesner slip factor. The compressor performance is evaluated using empirical correlations for compressor losses and flow deviation. The meanline program allows the calculation of the compressor map without increasing the time for the overall matching of the integrated system. Additionally, compressor geometry optimization can be performed not in isolation but in the frame of an integrated system. The geometry related inputs of the compressor code can be seen in Fig. 1.

The meanline code has been validated against experimental data published by NASA-Galvas (1973). As seen in Fig.2 and Fig. 3 the map derived for the specific geometry is in good agreement with the experimental data, especially for rotational speeds lower than the maximum one. The deviation between the experimental and calculated data increases as rotational speed increases, since at high rotational speeds the 3-D phenomena become significant. This error trend is similar to the original code presented by Galvas (1973). For surge line prediction, two surge criteria are taken into account, namely one for impeller inducer and one for vaned diffuser surge. Both surge limits are calculated with empirical correlations, developed by Rodgers (1963) and Galvas (1973) respectively.

Radial Inflow Turbine

Similar to the compressor, a meanline code based on the work of Wasserbauer et al. (1975) is used. In this meanline model, the flow properties are calculated along a streamline in mean radial position, computing turbine performance using empirical correlations for radial turbine losses and angle deviation. The geometry related inputs of the turbine code can be seen in Fig. 4. The code is validated against measured data for a specific geometry (Wasserbauer and Glassman, 1975). The results indicate that both chocking line and low pressure operating region are predicted with good accuracy, as seen in Fig. 5

Diesel Engine Model

For diesel engine modeling an in-house single zone thermodynamic combustion model has been used for the closed engine cycle. The main scope of the simulation model developed is to predict the engine performance, the thermodynamic properties of the working medium and its mass flow rate, in order to be coupled with the compressor and turbine model, using as little as possible experimental data for model calibration. Therefore, a simple approach is followed, which is based on the application of the first law of thermodynamics assuming that the entire combustion chamber consists of a single homogeneous mixed charge. Thus, only the temporal variation of the in-cylinder mixture concentration, temperature and thermodynamic properties is considered, as a function of the instantaneous cylinder volume. In other words, at each crank angle degree integration step, the model predicts the in-cylinder homogeneous mixture composition (i.e. perfect combustion products concentrations after combustion initiation), the in-cylinder pressure and the uniform in-cylinder bulk gas temperature. For the close part of engine cycle the energy conservation equation is written as:

$$\frac{dU_{cyl}}{dt} = \frac{dQ_w}{dt} + \frac{dQ_{comb}}{dt} - \frac{dW}{dt} \qquad (1)$$

The mechanical work performed by the piston during the compression and expansion phase is due to the volume change of the cylinder and is calculated by the following trapezoidal rule:

$$dW = (p_{cyl,i} + p_{cyl,i+1}) * \frac{dV_{cyl}}{2} \qquad (2)$$

where $p_{cyl,i}$ and $p_{cyl,i+1}$ are two successive values of cylinder pressure and dV_{cyl} is the cylinder volume step.

The heat addition via combustion is taken into account assuming complete combustion of the fuel injected with a specified lower heating value. The fuel burning rate at each crank angle degrees, is predetermined using a simple empirical model (Wiebe function) according to the following expression (Stiesch, 2003)

$$\frac{Q_{comb}(\varphi)}{Q_{comb,tot}} = 1 - \exp\left(-6.908 * \left(\frac{\varphi - \varphi_{SOC}}{\Delta\varphi_c}\right)^{m+1}\right) \qquad (3)$$

Where $Q_{comb,tot} = m_{fuel} * LHV$, m and $\Delta\varphi_c$ are parameters determined through the calibration procedure conducted. The ignition delay is estimated using an Arrhenius type equation (Heywood, 1988):

$$\tau_{id} = A * p_{cyl}^{-n} * exp\left(\frac{E_A}{\tilde{R}} * \frac{1}{T_{cyl}}\right) \qquad (4)$$

Where, P and T are the instantaneous in-cylinder pressure and temperature, E_A is the apparent activation energy of the fuel auto-ignition process, $\tilde{R}$ is the universal gas constant and A and n are constants dependent on the fuel. In this study the values proposed by Wolfer are used, i.e. n=1.19, A=0.44 and the parameter $E_A/\tilde{R}$=4650 K (Heywood, 1988).

The heat transfer between the cylinder gases and the combustion chamber walls can be due to both convection and solid body radiation which originates from hot soot particles. However, as stated in the model developed the assumption of ideally mixed combustion chamber is made, therefore, soot particles are not taken into account. To compensate this, the effect of radiative heat transfer is taken into account by an empirical augmentation of the convective heat transfer coefficient (Stiesch, 2003). The convective heat transfer rate between the gas and the wall can be described by the Newton's cooling law:

$$\dot{Q_w} = h * A * (T_w - T_{cyl}) \qquad (5)$$

Where h is the convective heat transfer coefficient, A is the instantaneous surface area of heat transfer and T_w, T_{cyl} are the mean wall and in-cylinder gas temperatures respectively. The convective heat transfer coefficient is estimated assuming that an analogy with a steady turbulent flow over a solid wall exists, using the following expression:

$$Nu = \frac{h * L}{k} = C * Re^{a} * Pr^{b} \qquad (6)$$

Where L represents a characteristic length and equals the cylinder bore diameter, C, a and b are empirical constants that are determined by curve fitting experimental data of wall heat transfer rates. In this study a=0.80, b=0.40. To calculate the brake engine power, the correlation proposed by Chen and Flynn (1965) for turbocharged engines are used, where the friction mean effective pressure FMEP in bar is calculated as:

$$FMEP = 0.137 + 0.005 * P_{max} + 0.162 * c_{piston,mean} \qquad (7)$$

Where P_{max} is the peak combustion in-cylinder pressure in bar and $c_{piston,mean}$ is mean piston speed in m/s. The air mass flow rate is calculated using the following expression:

$$\dot{m}_{AIR} = \frac{P_{im}}{R * T_{im}} * V_{sw} * n_{vol} * (\frac{N}{2}) \qquad (8)$$

Where P_{im} and T_{im} are the pressure and temperature at the engine inlet manifold (after inter-cooler), n_{vol} is the volumetric efficiency, R is the air gas constant and N is the engine crankshaft speed. The gas temperature at IVC is calculated using the following equation:

$$T_{IVC} = T_{im} + \Delta T \qquad (9)$$

Where ΔT is an adjusted input parameter to the integrated simulation model.

The volumetric efficiency n_{vol} used in Eq. (8) is adjusted in order predicted data for peak cylinder pressure, brake power output and exhaust gas temperature after turbocharger to match corresponding shop trials data. The exhaust gas flow rate is calculated by:

$$\dot{m}_{EXH} = \dot{m}_{AIR} + \dot{m}_{fuel} \qquad (10)$$

A polytropic expansion is used to calculate exhaust gas temperature using corresponding value of exhaust gas temperature at EVO as follows:

$$T_{exh} = T_{EVO} \left(\frac{P_{exh,manif}}{P_{EVO}}\right)^{\frac{n-1}{n}} \qquad (11)$$

Where P_{EVO} is the cylinder gas pressure at EVO and $P_{exh,manif}$ is the exhaust manifold pressure, which is calculated using the following expression:

$$P_{exh,manif} = \frac{1}{2}P_{im} + \sqrt{(P_{im}100)^2 - 8\dot{m}_{exh}^2 T_{im} + (T_{EVO} - T_{im})} \qquad (12)$$

At this point it is worth to make some observations about the diesel engine closed-cycle simulation model. Specifically, the model predicts the variation of in-cylinder pressure during closed-cycle diesel engine operation and thus, it does not account for the variation of cylinder pressure during intake stroke in order to calculate the pumping work during gas exchange. However, the impact of the negative pumping power on the brake engine power output is rather limited since the highest portion of indicated power results from the closed-cycle engine operation and thus, the error induced in the calculation is not considerably important. The results from a more detailed phenomenological model which is under development, considering the time and space evolution of the fuel jet, along with cylinder pressure predictions during gas exchange process, will be presented in a future paper. However, it should be underlined that the main scope of the selection of single-zone approach was based on the fact that it is suitable for cases where there are very limited available data for the geometrical and the operational characteristics of the engine. This is the case that is usually met in practical applications where turbo-matching has to be implemented in existing engines under retrofitting (i.e. replacement of existing turbocharger with another one) where the only available data are the test records of the diesel engine at shop trials.

Intercooler

The intercooler performance is estimated by prescribing the intercooler effectiveness and total pressure losses on the hot and cold sides. The temperature effectiveness (ε) and pressure drop at design point are defined according to the following equations (Alexiou and Tsalavoutas, 2013).

$$\varepsilon = \frac{T_{in,hot} - T_{out,hot}}{T_{in,hot} - T_{in,cold}} \qquad (13)$$

$$P_{out,cold\ or\ hot} = P_{in,cold\ or\ hot}(1 - dP_{cold\ or\ hot}) \qquad (14)$$

Where $dP_{cold\ or\ hot}$ is the pressure drop in the intercooler. In order to estimate the outlet temperatures of both cold and hot side of the intercooler, a heat flow balance is performed between the hot and cold

sides. For off-design operation the pressure drop is a function of mass flow deviating relative to design as is the effectiveness (Walsh and Fletcher, 2008).

Coupling between T/C and Diesel Engine

CC and RT geometries are used as input data for the meanline models in order corresponding performance maps to be generated. The input data for diesel model set up are the inlet valve closing angle, the exhaust valve opening angle, the compression ratio, the cylinder bore, the piston stroke, the generator efficiency and the shop trials data. The input data for intercooler model set up are the inlet air mass flow, pressure drop and effectiveness at nominal point (100% of load). Having established the integrated model for a specific turbocharged diesel engine, the required input data for a single operating point run are ambient conditions, engine speed and engine fuel consumption (or demanded output power). This procedure flow chart is depicted in Fig. 6.

Test Case Engine

The present integrated simulation platform is used to simulate the operation of a specific turbocharged marine diesel engine throughout its whole operating envelope. The technical specifications of the diesel engine are shown in Table 1.

The results are compared against engine shop trials data for validating the overall system model. The shop trials data are shown in Table 2.

Experimental Verification

As discussed, the approach followed for the simulation of diesel engine operation is based on empirical and semi-empirical expressions to determine the fuel burning rate, heat transfer and friction power losses. Therefore, it is necessary to calibrate model's constants by comparing the output of the simulation model with corresponding available experimental data. It should be noticed, that since the original scope of the simulation framework was to be used as a tool in retrofitting existing engines, the data used for model calibration are limited to the ones usually found in shop test records, which for the case examined are: engine brake power output, peak in-cylinder combustion pressure and exhaust gas

317 temperature. The values of the calibration constants are determined following an optimization procedure
318 to minimize the error when comparing calculated and measured values at each operating point (25%,
319 50%, 75% and 100% of full engine load) and at rated engine speed.

320 In Fig. 7 the comparison between the measured and the calculated values for brake engine power,
321 peak combustion pressure and exhaust gas temperature, at the engine operating conditions used for
322 calibration is depicted. As observed, there is a good matching between measured and calculated values,
323 which indicates that the model reliably reproduce the specific engine operation for the entire range of the
324 conditions examined. It should be noted that one set of calibration parameters is used for the whole
325 operating envelope.

326 **Turbocharged Engine model validation with Engine shop trials**

327 The geometry of the compressor and turbine has been measured and used as input to the mean line
328 compressor and turbine codes. The specific fuel consumption and boost pressure against engine power is
329 presented in Fig. 8 for five different operating points (Load: 25, 50, 75, 100 and 110%) as reported in the
330 engine shop trials.

331 As seen, the integrated turbocharged engine model simulates the overall engine operation in very
332 good agreement to the engine shop trials data. The maximum deviation from the reported mean sfc and
333 boost pressure value is 2.6% and 9% respectively. It should be noted that the reported at the shop trials
334 maximum measurement error for the sfc is 5%. The matching of T/C components with engine is
335 presented in Fig. 9 and Fig. 10 where the compressor and turbine maps with corresponding operating
336 lines are shown.

337 Having established a model that can simulate the turbocharged engine throughout its operating
338 envelope the effect of specific faults on performance and operability can be assessed and the system
339 behavior can be analyzed. Specifically, T/C components and heat exchanger fouling is examined herein.

340 **Turbocharger fouling assessment**

341 Turbocharger fouling can be caused due to compressor fouling, turbine fouling or a combination of
342 both, leading to inefficient operation and a shift of operating and surge line. All compressors are

susceptible to fouling as a result of the ingestion of air impurities that accumulate on and stick to gas path free surfaces, blades and shrouds, modifying airfoil geometry (Diakunchak, 1992). In addition, oil leaks from compressor seals and bearings mix with some of the ingested particles and deposit on the blade surfaces (Lakshminarasimha et al. 1994). The result will be the deterioration of airfoils aerodynamic behavior and reduction of flow area leading to the compressor and engine performance degradation.

Turbine fouling is mainly depending on type and quality of the operating fuel as discussed by Meher-Homji (1987). When heavy fuel oil or crude oil is used, the turbine degradation is expected to be significant. Low melting point ashes, metals and unburned hydrocarbons can be aggregated in the turbine in the form of scale. The contaminants deposition will have an impact over blade, by changing the airfoil shape, the inlet angle and increasing the surface roughness. These effects will result to the reducing of the airfoil throat area and apparently reducing the performance characteristics and the service life of the component. Also, especially in marine gas turbines, sulfidation may occur resulting in turbine corrosion. As a result, fouling rate will increase, as discussed by Basendwah et al. (2006)

Since both T/C components may be fouled, five different fouling cases are simulated herein. The simulation is performed by altering the blade thickness and friction accordingly, as presented in Table 3. The selected blade thickness change due to fouling is between 0.2 and 0.5 mm as proposed by Mezheritsky and Sudarev(1990) for a medium size T/C.

The results of fouling analysis are shown in Fig11 –Fig13. As seen in Fig. 11, compressor fouling causes the movement of the surge line towards lower pressure ratios for high rotational speeds, hence reducing the compressor stable operation regime. Turbine fouling is mostly affecting the inlet mass flow and turbine efficiency hence reducing shaft horse power and increasing specific fuel consumption. As seen in Fig. 12 the fifth simulated case (F2-F3), which is the most severe one, results to a shaft horse power reduction of 22% highlighting the effect that T/C components fouling can have on a turbocharged engine. For this reason the original nominal power demand canot be satisfied for this case.The effect of fouling on fuel consumption is considerable leading to a specific fuel increase of about 5% for the worst case, as depicted in Fig. 13.

For further interpretation of the fouling analysis, additional simulation is performed, with results presented in Table 4 highlighting the effect of fouling in engine performance degradation for constant engine speed and load. The demanded shaft power, used in this simulation, represents the fifth simulated case (F2-F3) maximum power, aiming to ensure that engine operates stable in all fouling conditions. It is observed that as the fouling level increases, the fuel consumption increases in order to satisfy the demanded load. Also boost pressure and T/C rotational speed reduction occurs due to compressor and turbine degradation. Final, the system outlet temperature rises, because of the turbine efficiency reduction.

Intercooler fouling assessment

The air density determines the maximum weight of fuel that can be effectively burned per working stroke in the cylinder. The increase in air density can be performed by decreasing the charged temperature leading to power increase. The intercooling is used for this purpose. In most cases, intercooler consists of three channels.

- Air channel
- Brackish water channel
- Sea water channel

Brackish water drains heat energy from charged air through a finned tube exchanger, increasing its density. This energy is transferred in next step to sea water through a secondary exchanger. In order to perform the simulation of a fouled intercooler it was assumed that:

- Maximum fouling sea water resistance is $0.176\ m^2K/kW$ (Kakac et al. 2012)
- Maximum pressure drop increase is 0.29% due to fouling. (Gautam et al. 2017)

Using the heat exchanger fouling assumptions, clean cooler effectiveness to fouled cooler effectiveness ratio can be determined as follows.

$$\frac{\varepsilon_{\text{clean}}}{\varepsilon_{\text{fouled}}} = \frac{\frac{1}{U_{\text{clean}}} + R_f}{\frac{1}{U_{\text{clean}}}} \quad (15)$$

Thus, calculating ε_{fouled} and using it, in turbocharged engine model, sfc, power and temperature changes can be calculated. Heat exchanger fouling leads to effectiveness reduction and pressure drop increase, hence, the air density before the manifold is decreased causing engine shaft horse power and efficiency reduction. The fuel consumption is increased by 1% as reported in Table 5, thus heat exchanger fouling economic effect can become significant. In addition exhaust gas temperature increases significant and turbocharger operating line is moved towards surge (Fig. 14), expected to affect turbocharger stable operation.

The heat exchanger fouling rate depends on many parameters, including time. It is of interest to assess how the buildup of heat exchange fouling affects the overall turbocharged engine performance over time. The changes of pressure drop and resistance over time are evaluated according to the following and the values discussed, while time is assumed dimensionless, for expressing the relative change of performance parameters over time (see Fig 15 and Fig 16).

- Pressure drop reduction function against fouling resistance has parabolic form. (Gautam et al. 2017)
- Fouling resistance function against time has linear form. (Kakac et al. 2012)

As seen in Fig. 16 the sfc increase and the shaft horse power decrease are more profound during the first period of fouling. Over time the fouling build up is degrading the overall performance but the degradation rate is expected to be reduced over time.

Conclusion

An integrated simulation framework for turbocharged internal combustion engine performance and operability assessment has been developed. For the turbomachinery components 1D models have been applied for analyzing the impact of turbomachinery fouling on sub-system and system level. The effect of

intercooler fouling has been assessed as well. The assessment is undertaken utilizing models suitable adapted to shop trials data. The results indicate that:

Compressor fouling causes the movement of the surge line towards lower pressure ratios, hence reducing the compressor stable operation regime. Turbine fouling is mostly affecting the inlet mass flow and turbine efficiency reducing shaft horse power and increasing specific fuel consumption. As for the combination of compressor and turbine fouling, power may be reduced up to 22% highlighting the effect that T/C components fouling can have on a turbocharged engine and leading to a 5% specific fuel consumption increase.

Heat exchanger fouling leads to effectiveness reduction and pressure drop increase resulting, for the case examined herein, to 1% specific fuel consumption increase and 1% power decrease, indicating that intercooler fouling may affect the engine life cycle cost. In addition exhaust gas temperature increases significant, an increase that is expected to affect the turbocharger bearings life. Also, turbocharger operating line is moved towards surge line, increasing the chance of working under unstable operation.

The present simulation framework has a lot of possible other applications apart from the study of engine system degradation due to fouling in T/C components and heat exchanger. It can be an integrated part either of a retrofitting platform with design and optimization modules or of a diagnostic tool, for predictive maintenance purposes. Therefore, the authors intent to replace the single-zone diesel engine model by a more detailed phenomenological one coupled with detailed modeling for NOx emissions from marine diesel engine, while CO2 emissions will be directly calculated by the fuel consumption.

Finally, the present framework can be used to any type of turbocharged engine after specific modifications, which include adaptation of engine modeling to gasoline or diesel engine geometrical and operational specifications and individual combustion conditions. The single-zone combustion model modifications for gasoline engines include the selection of a Wiebe function suitable for gasoline combustion and the observation of cylinder pressure variation rate for controlling fuel supply to avoid pre-ignition or post-combustion knocking phenomena. Single-zone combustion concept can be considered more suitable for gasoline combustion modeling due to its predominantly premixed nature.

Data Availability

All the data generated or used during the study are available from the corresponding author by request.

References

Alexiou A., Roumeliotis I., Aretakis N., Tsalavoutas A. and Mathioudakis K. (2012). "Modelling Contra-Rotating Turbomachinery components for engine performance simulations: The geared turbofan with Contra-Rotating core case". *ASME J. Eng. Gas Turbines Power, 134(11): 111701 (10 pages).*

Alexiou, A. and Tsalavoutas, A. (2013). *Turbo 3.2 Library Reference Manual.* Madrid: Empresarios Agrupados Internacional S.A.

Aungier, R.H. (1995). "Mean streamline aerodynamic performance analysis of centrifugal compressor". *ASME J. Turbomach*, 117(3): 360-366 (7 pages).

Baldi, F., Theotokatos, G, and Andersson, K. (2015). "Development of a combined mean value-zero dimensional model and application for a large marine four-stroke Diesel engine simulation." *Applied Energy* 154, 402-415. doi:https://doi.org/10.1016/j.apenergy.2015.05.024

Barelli, L., Bidini, G. and Bonucci, F. (2009). "Diagnosis methodology for the turbocharger groups installed on a 1 MW internal combustion engine." *Applied Energy* 86(12), 2721–2730. https://doi.org/10.1016/j.apenergy.2009.04.034

Basendwah, A., Pilidis, P. and Li, Y.G. (2006). "Turbine Off- Line Water Wash Optimization Approach for Power Generation." Proceeding of ASME Turbo expo, Barcelona, Spain, 8-11 May, GT2006-90244, pp. 65-76; 12 pages.

Bricknell, D.J. (2006). "Marine Gas Turbine Propulsion System Application." Proceeding of ASME Turbo Expo, Barcelona, Spain, 8-11 May, GT2006-90751.

Button, R.W., Martin, B., Sollinger, J. and Tidwell, A. (2015). "Assessment of Surface Ship Maintenance Requirements." CA: RAND Corporation,. https://www.rand.org/pubs/research_reports/RR1155.html. Also available in print form..

469 Catania, A.E., Finesso, R., and Spessa, E. (2011). "Predictive Zero-Dimensional Combustion Model for
470 DI Diesel Engine Feed-Forward Control." *Energy Conv. Manageme.* 52(10), 3159-3175.
471 doi:10.1016/j.enconman.2011.05.003
472 Charlton, S.J. (1992). "SPICE - Simulation program for internal combustion engines." User Manual
473 (University of Bath).
474 Chen, S. and Flynn, P. (1965). "Development of a Single Cylinder Compression Ignition Research
475 Engine." SAE Technical Paper 650733, SAE, Warrendale, PA, pages 14.
476 doi:https://doi.org/10.4271/650733
477 Cui, X., Yang, C., Serrano, J., and Shi, M. (2018). "A performance degradation evaluation method for a
478 turbocharger in a diesel engine." *R. Soc. Open Sci.* 5: 181093.
479 doi:http://dx.doi.org/10.1098/rsos.181093
480 Diakunchak, I. S. (1992). "Performance Deterioration in Industrial Gas Turbines." *ASME J. Eng. Gas*
481 *Turbines Power, 114(2): 161-168 (8 pages).*
482 Galvas, M.R. (1973). "Fortran program For predicting off design performance of Centrifugal
483 Compressor." NASA TN D-7487.
484 Giakoumis, E.G., Dimaratos, A.M., Rakopoulos, C.D., and Rakopoulos, D.C. (2017) "Combustion
485 instability during starting of turbocharged diesel engine including biofuel effects", *J. Energy*
486 *Engineering, ASCE,* 143(2), 04016047. DOI: 10.1061/(ASCE)EY.1943-7897.0000402
487 Giakoumis, E.G., and Tziolas, V. (2018) "Modeling a variable-geometry turbocharged diesel engine under
488 steady-state and transient conditions", *J. Energy Engineering, ASCE,* 144(3), 04018017, DOI:
489 10.1061/(ASCE)EY.1943-7897.0000537.
490 Guatam, K-R., Parmar, N., and Vyas, B. (2017) "Effect of fouling on thermal and hydraulic parameter of
491 Shell and Tube Heat exchanger", Student conference 2017, Czech Technical University, At
492 Prague, Czech Republic
493 Heywood, J. B. (1988). *Internal combustion engine fundamentals.* McGraw-Hill, New York.

494 Huang, L., Ma, C., Li, Y., Gao, J., and Qi, M. (2018) "Applying neural networks (NN) to the
495 improvement of gasoline turbocharger heat transfer modeling", *Applied Thermal Engineering*,
496 141, 1080-1091, https://doi.org/10.1016/j.applthermaleng.2018.06.062.
497 Japikse, D. (1996). Centrifugal Compressor Design and Performane. *3rd ed., Concepts ETI Inc.:*
498 *Wilder,TN, USA, pp. 2.26–2.81.*
499 Japikse, D., and Baines, N.C. (1997). *Introduction to Turbomachinery.* Concepts ETI Inc and Oxford
500 University Press.
501 Kakac, S., Liu, H., and Pramuanjaroenkij, A. (2012). *Heat Exchangers.* CRC Press.
502 Kökkülünk, G., Parlak, A., and Erdem, H-H. (2016) "Determination of performance degradation of a
503 marine diesel engine by using curve based approach", *Applied Thermal Engineering*, 108, 1136-
504 1146, http://dx.doi.org/10.1016/j.applthermaleng.2016.08.019.
505 Kowalski, J. (2015) "Concept of the multidimensional diagnostic tool based on exhaust gas composition
506 for marine engines", *Applied Energy* 150, 1-8. https://doi.org/10.1016/j.apenergy.2015.04.013
507 Kurz, R., and Brun, K. (2009). "Degradation of gas turbine performance in natural gas service." *Journal*
508 *of Natural Gas Science and Engineering*, 1, 95–102. doi:10.1016/j.jngse.2009.03.007
509 Kurzke, J. (1996). "How to get Component Maps for Aircraft Gas Turbine Performance Calculations."
510 Proceeding of ASME Turbo Expo, Birmingham, UK, 96-GT-164, 2-5 June, 7 pages
511 Lakshminarasimha, A.N., Boyce, M.P., and Meher-Homji, C.P. (1994). "Modelling and Analysis of Gas
512 Turbine Performance Detrerioration." *ASME J. Eng. Gas Turbines Power,* 116(1), 46-52.
513 https://doi.org/10.1115/1.2906808
514 Ledger, J.D., Benson, R.S., and Furukawa, H. (1973). "Improvements in transient performance of a
515 turbocharged diesel engine by air injection into the compressor." *SAE Paper No. 730665*, SAE,
516 Warrendale, PA. https://doi.org/10.4271/730665.
517 Ledger, J.D., and Walmsley, N.D. (1971). "Computer simulation of a turbocharged diesel engine
518 operating under transient load conditions." *SAE Paper No. 710117*, SAE, Warrendale, PA.
519 Liang, L., Naik, C., Puduppakkam, K., Wang, C., Modak, A., Meek, E., Ge, H., Reitz, R., and Rutland,
520 C. (2010). "Efficient Simulation of Diesel Engine Combustion Using Realistic Chemical Kinetics

521 in CFD." *SAE Paper No. 2010-01-0178,* SAE, Warrendale, PA doi:https://doi.org/10.4271/2010-
522 01-0178
523 Meher-Homji, C.B . (1987). "Compressor and Hot Section Fouling in Gas Turbines – Causes and
524 Effects." *Proceedings of the 9th Industrial Energy Technology Conference.* Houston: Texas A&M
525 University.
526 Melino, M., Morini, M., Peretto, A., Pinelli, M., and Spina, P.R. (2011). "Compressor Fouling Modeling:
527 Relationship Between Computational Roughness and Gas Turbine Operation Time." *Proceeding*
528 *of ASME Turbo Expo*, Vancouver, British Columbia, 6-10 June.
529 Mezheritsky, A.D., and Sudarev, A.V. (1990). "The mechanism of fouling and the cleaning technique in
530 application to flow parts of the power generation plant compressors." *Proceeding of ASME Turbo*
531 *Expo*, Brussels, Belgium, 90-GT-103, 11-14 June.
532 Murphy A.J., Norman, A.J., Pazouki, K., and Trodden, D.G. (2015). "Thermodynamic simulation for the
533 investigation of marine Diesel engines." *Ocean Engineering*, 102, 117-128.
534 https://doi.org/10.1016/j.oceaneng.2015.04.004
535 Pagán Rubio, J.A., Vera-García, F., Hernandez Grau, J., Muñoz Cámara, J., and Albaladejo Hernandez, D.
536 (2018). "Marine diesel engine failure simulator based on thermodynamic model." *Applied*
537 *Thermal Engineering.*, 144, 982-995. doi:https://doi.org/10.1016/j.applthermaleng.2018.08.096
538 Pariotis, E. and Hountalas, D. (2003). "A New Quasi-Three Dimensional Combustion Model for
539 Prediction of DI Diesel Engines' Performance and Pollutant Emissions." *SAE Transactions, J.*
540 *Engines,* 112, 1417-1429 . doi:https://doi.org/10.4271/2003-01-1060
541 Pariotis, E. and Hountalas, D. (2004). "Validation of a Newly Developed Quasi-Dimensional Combustion
542 Model - Application on a Heavy Duty DI Diesel Engine." *SAE Paper 2004-01-0923*, SAE,
543 Warrendale, PA, Pages 15. doi:https://doi.org/10.4271/2004-01-0923
544 Pariotis, E., Hountalas, D., and Rakopoulos, C. (2005). "Modeling the Effects of EGR on a Heavy Duty
545 DI Diesel Engine Using a new Quasi-Dimensional Combustion Model." *SAE Paper 2005-01-*
546 *1125*, SAE, Warrendale, PA, Pages 20. https://doi.org/10.4271/2005-01-1125

547 Pesiridis A., Salim, W., and Martinez-Botas, R.F. (2012). *Turbocharger Matching Methodology for*
548 *Improved Exhaust Energy Recovery*. 10th International Conference on Turbocharging and
549 Turbochargers of the IMechE. Woodhead Publishing, 456 pages.
550 Petranović, Z., Sjerić, M., Taritaš, I., Vujanović, M., and Kozarac, D. (2018). "Study of advanced engine
551 operating strategies on a turbocharged diesel engine by using coupled numerical approaches."
552 *Energy Convers. Manage.*, 171, 1-11. doi:https://doi.org/10.1016/j.enconman.2018.05.085
553 Qiu, X., Fredriksson, C.F., Baines, N.C., and Backlund, M. (2013). "Designing turbochargers with an
554 integrated design system." *Proceedings of ASME Turbo Expo*, San Antonio, Texas, USA, 3-7 June,
555 GT2013-94894.
556 Rakopoulos, C.D., Rakopoulos, D.C., and Giakoumis, E.G. (2015). "Impact of properties of vegetable oil,
557 bio-diesel, ethanol and n-butanol on the combustion and emissions of turbocharged HDDI diesel
558 engine operating under steady and transient conditions." *Fuel* 156, 1-19.
559 https://doi.org/10.1016/j.fuel.2015.04.021
560 Rakopoulos, C.D., Rakopoulos, D.C., Kosmadakis, G.M., and Papagiannakis, R.G. (2019). "Experimental
561 comparative assessment of butanol or ethanol diesel-fuel extenders impact on combustion
562 features, cyclic irregularity, and regulated emissions balance in heavy-duty diesel engine." Energy
563 174, 1145-1157. https://doi.org/10.1016/j.energy.2019.03.063
564 Rakopoulos, C.D., Rakopoulos, D.C., and Kyritsis, D.C. (2003). "Development and validation of a
565 comprehensive two-zone model for combustion and emissions formation in a DI diesel engine."
566 *Int. J. Energy Res.* 27(14), 1221-1249. https://doi.org/10.1002/er.939
567 Rakopoulos, C.D., Rakopoulos, D.C., Mavropoulos, G.C., and Kosmadakis, G.M. (2018). "Investigating
568 the EGR rate and temperature impact on diesel engine combustion and emissions under various
569 injection timings and loads by comprehensive two-zone modeling." *Energy* 157, 990-1014.
570 https://doi.org/10.1016/j.energy.2018.05.178
571 Reitz, R.D., and Rutland, C.J. (1995). "Development and testing of diesel engine CFD models." *Progress*
572 *in Energy and Combustion Science*, 21, 173-196. doi:https://doi.org/10.1016/0360-
573 1285(95)00003-Z

574 Rodgers, C. (1963). “Typical Performance Characteristics of Gas Turbine Radial Compressors.” *ASME J.*
575 *Eng. Power.* Apr 1964, 86(2): 161-170 (10 pages).
576 Romagnoli, A. and Martinez-Botas, R. (2011). “Performance Prediction of a Nozzled and Nozzleless
577 Mixed-flow.” *Int. J. Mechanical Sciences*, 53(8):557-574.
578 Sakellaridis, N. and Hountalas, D. (2013). “Meanline Modeling of Radial Turbine Performance for
579 Turbocharger Simulation and Diagnostic Applications.”, *SAE Technical Paper 2013-01-0924*,
580 SAE, Warrendale, PA, Pages 13. doi:https://doi.org/10.4271/2013-01-0924
581 Sakellaridis, N.F., Raptotasios, S.I., Antonopoulos, A.K., Mavropoulos, G.C. and Hountalas, D.T. (2015)
582 “Development and validation of a new turbocharger simulation methodology for marine two
583 stroke diesel engine modelling and diagnostic applications”, *Energy*, 91, 952-966,
584 http://dx.doi.org/10.1016/j.energy.2015.08.049
585 Stiesch, G. (2003). *Modeling Engine Spray and Combustion Processes. Heat and Mass Transfer.* Springer
586 Berlin Heidelberg, Berlin, Heidelberg.
587 Stuart S., Spence S., Filsinger D., Starke A., Kim S. K. (2017). “Characterising the influence of impeller
588 exti recirculation on Centrifugal Compressor work input.” *Proceeding of ASME Turbo Expo*,
589 Charlotte, NC, USA, 26-30 June, GT2017-63047.
590 Walsh, P.P. and Fletcher, P. (2008). *Gas Turbine Performance (second edition).* Blackwell Science Ltd.
591 Wasserbauer C.A., and Glassman C.A. (1975). *Fortran Program for predicting off-design performance of*
592 *Radial-Inflow Turbines.* NASA TN D-8063.
593 Watson, N. and Janota, M.S. (1982). *Turbocharging the Internal Combustion Engine.* McMillan Ltd.,
594 doi:https://doi.org/10.1007/978-1-349-04024-7
595 Watson, N. and Marzouk, M. (1977). “A non-linear digital simulation for turbocharged diesel engines
596 under transient conditions”, *SAE Technical Paper 770123*, SAE, Warrendale, PA.

Table 1 Click here to access/download;Table;Table1.docx

Table 1. Diesel engine technical specifications

Cycle	4	Fuel LHV [kJ/kg]	42700
Cylinders	5	Number of turbochargers	1
Bore[mm]	200	Injection timing	10 degCA BTDC
Stroke[mm]	300	Injection pressure	294 bar
Fuel Type	Diesel	Number of injector nozzle holes	8

Click here to access/download;Table;Table2.docx

Table 2. Diesel engine shop trials data

Load [%]	Output [kW]	Fuel* [kg/h]	C.P [barg]	C.T [C]	P_{amb} [mbar]	T_{amb} [C]	RH [%]	P_{max} [bar]	T_{exh} [C]
25	113	32.2	0.36	35	1001.5	31	62	62	283
50	225	53.5	0.69	37	1003.7	30.5	66	83	339
75	338	73.6	1.23	42	1003.5	31	65	108	365
100	450	94.5	1.84	45	1003	31.5	59	131	399
110	495	104.3	2.05	47	1002.7	32.5	54		

Click here to access/download;Table;Table3.docx

Table 3. Turbocharger fouling conditions

	Centrifugal Compressor			Radial Turbine		
Fouling condition	Blade thick. change[mm]	Blade thick. change [%]	Friction coef. change [%]	Nozzle thick. change [mm]	Nozzle thick. change [%]	Friction Coef. change [%]
F1	+0.2	+21%	+13%	-	-	-
F2	+0.5	+54%	+50%	-	-	-
F3	-	-	-	+0.5	-2.4%	+37.5%
F1-F3	+0.2	+21%	+13%	+0.5	-2.4%	+37.5%
F2-F3	+0.5	+54%	+50%	+0.5	-2.4%	+37.5%

Click here to access/download;Table;Table4.docx

Table 4. System operation dependence on fouling

Fouling condition	Specific shaft horse power (377 kW)				
	T/C rotational speed	Boost Pressure	T4	T5	sfc
F1	-0.9%	-10.0%	3%	4%	0.28%
F2	-2.0%	-22.2%	8%	12%	1.06%
F3	-2.2%	-6.2%	2%	4%	0.17%
F1-F3	-2.6%	-13.9%	5%	8%	0.61%
F2-F3	-3.7%	-26.1%	9%	15%	1.31%

Click here to access/download;Table;Table5.docx

Table 5. Fouled intercooler parameters

Condition	sfc [g/kWh]	T4 (ºC)	T5 (ºC)
Healthy	214.49	480	360
Fouled Intercooler	216.72 (+1.04%)	497 (+17)	381 (+21)

Figure 1

Click here to access/download;Figure;Fig1.tif

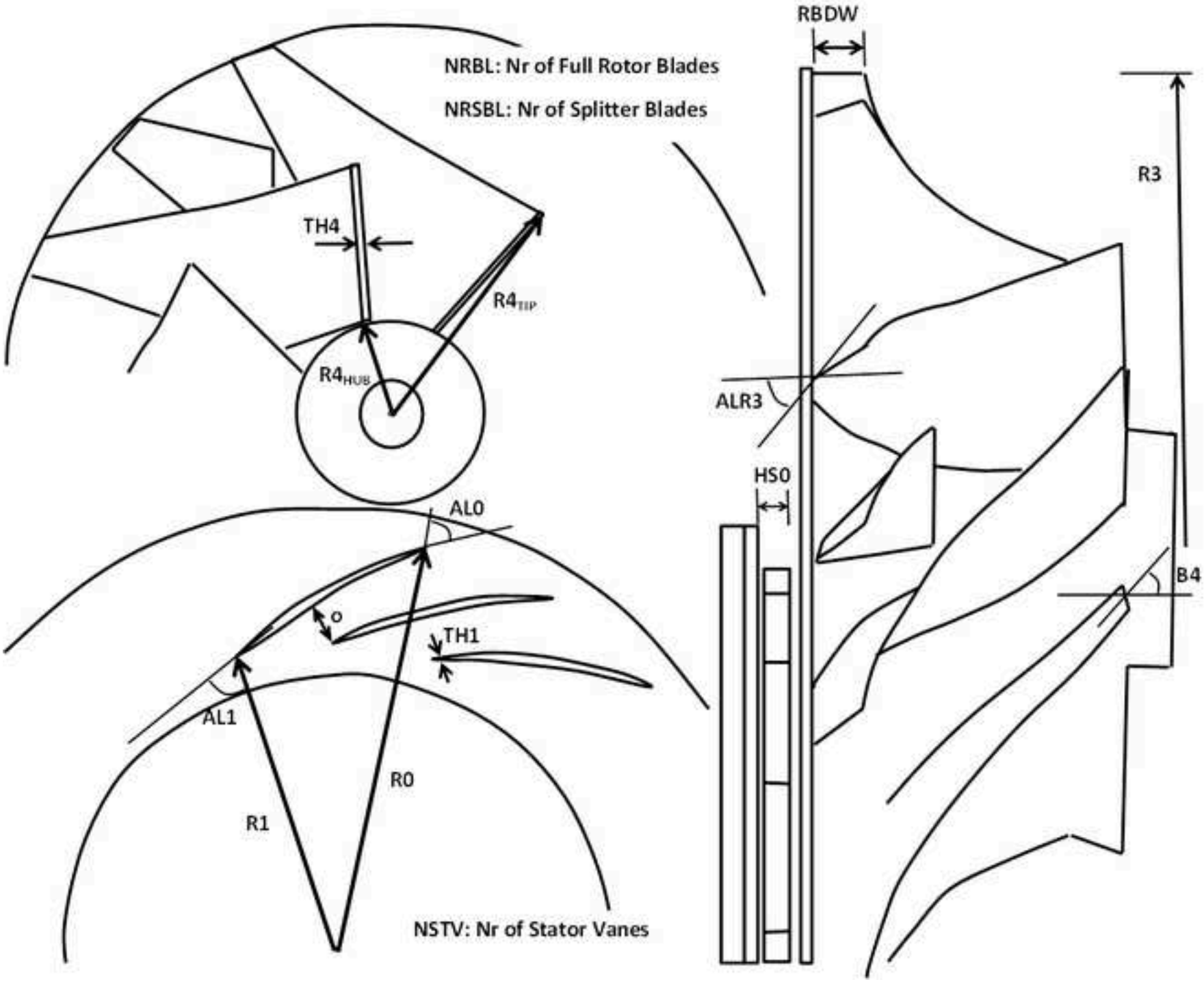


Figure 2

Click here to access/download;Figure;Fig2.tif

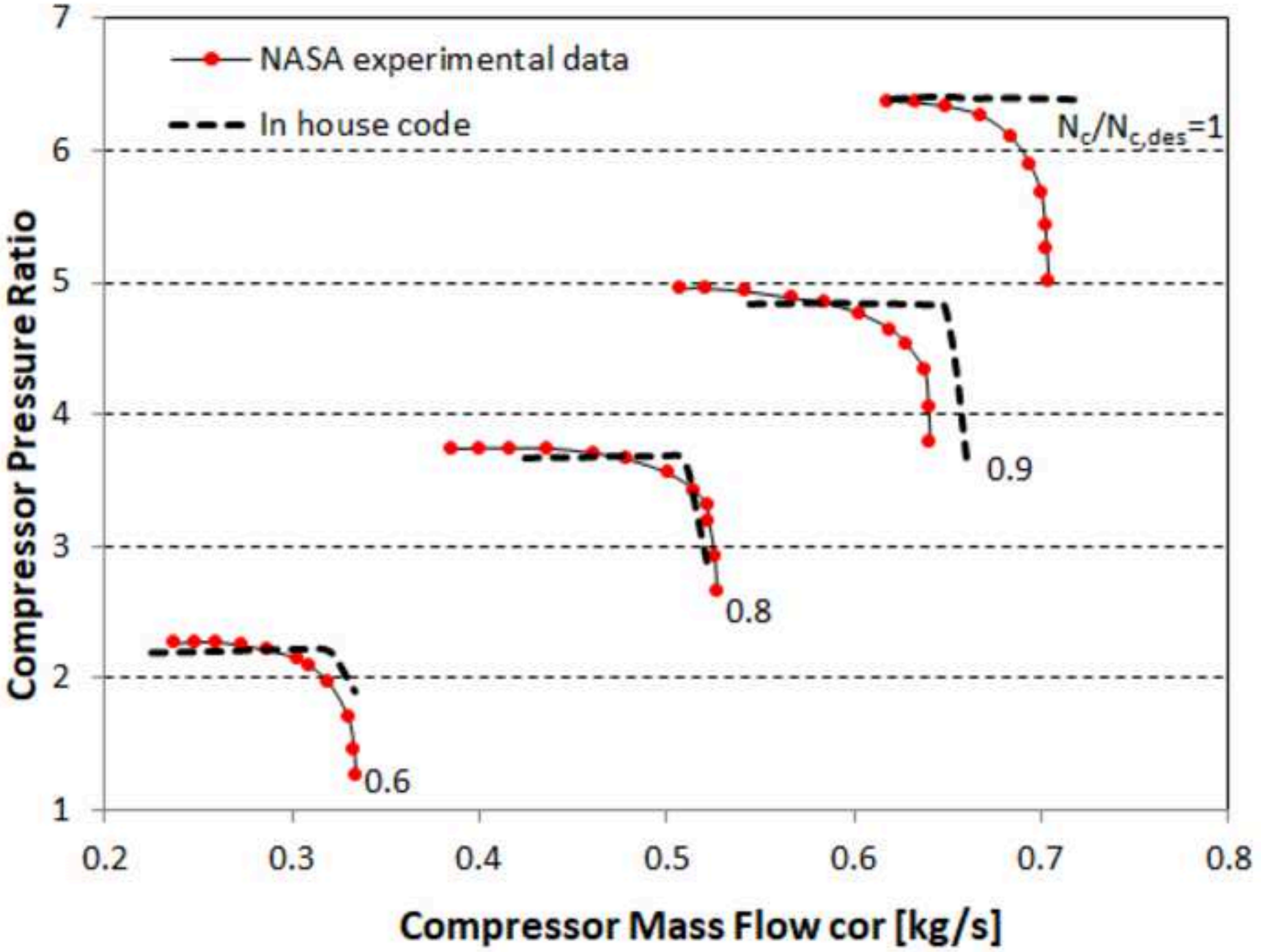


Figure 3

Click here to access/download;Figure;Fig3.tif

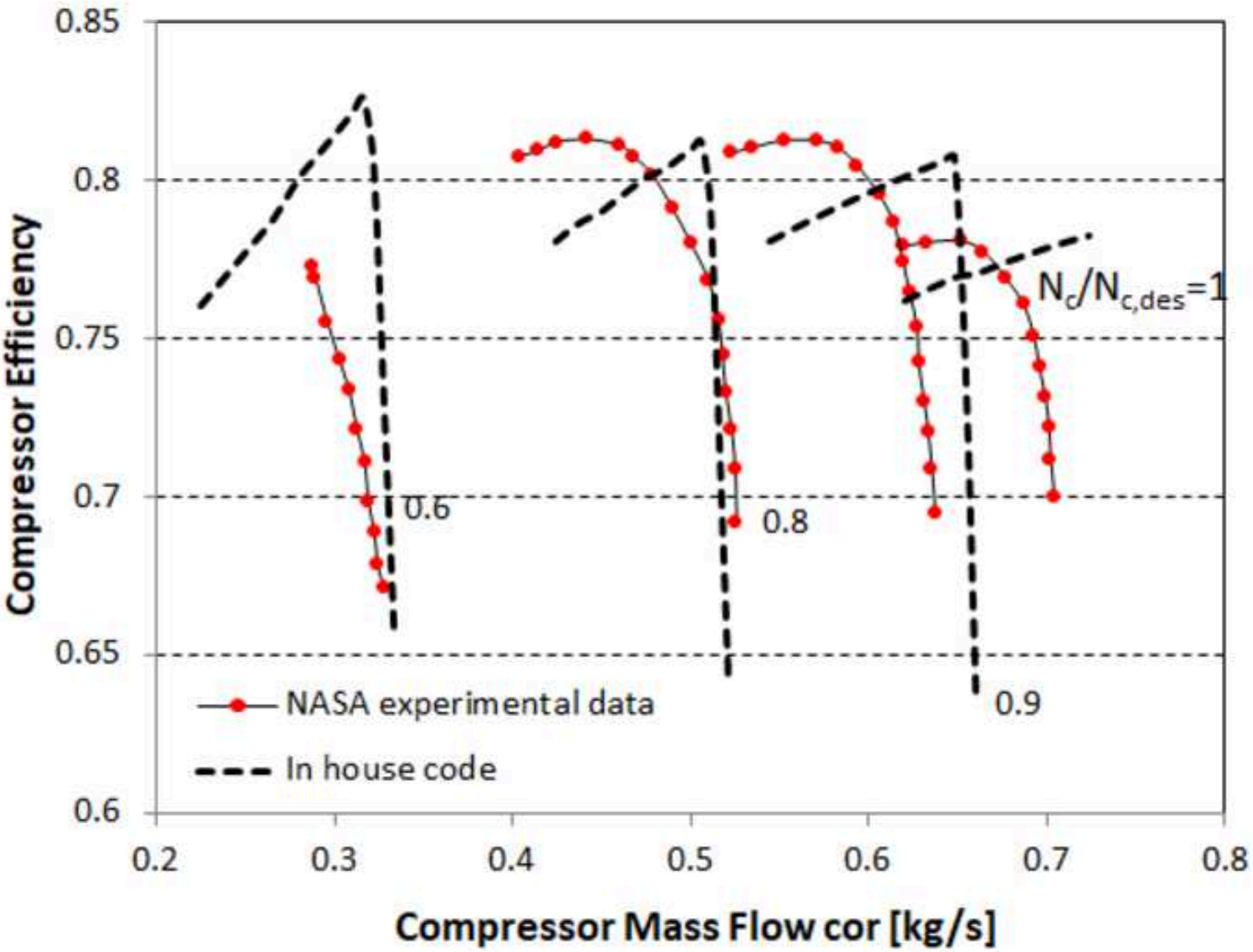


Figure 4

Click here to access/download;Figure;Fig4.tif

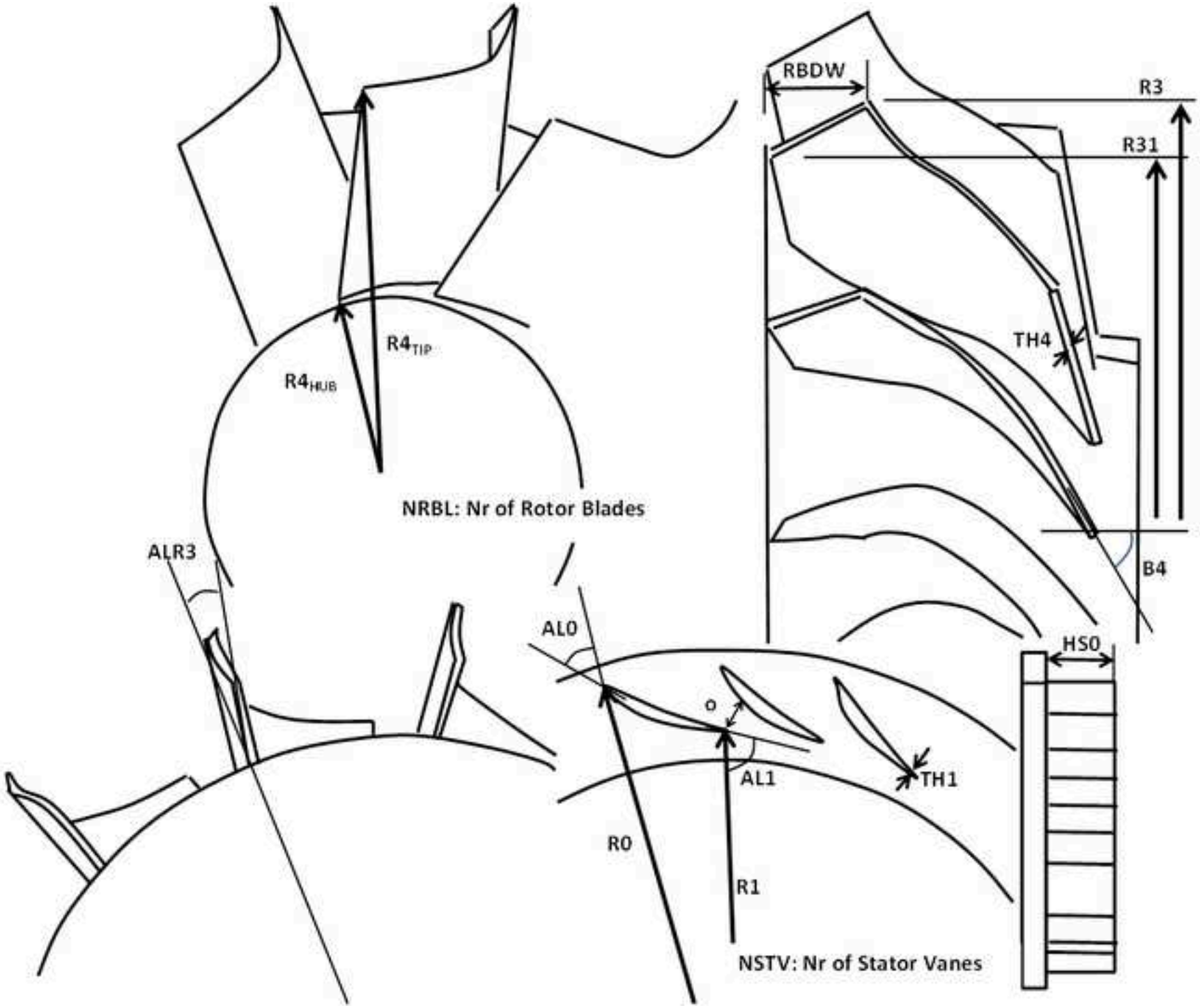


Figure 5

Click here to access/download;Figure;Fig5.tif

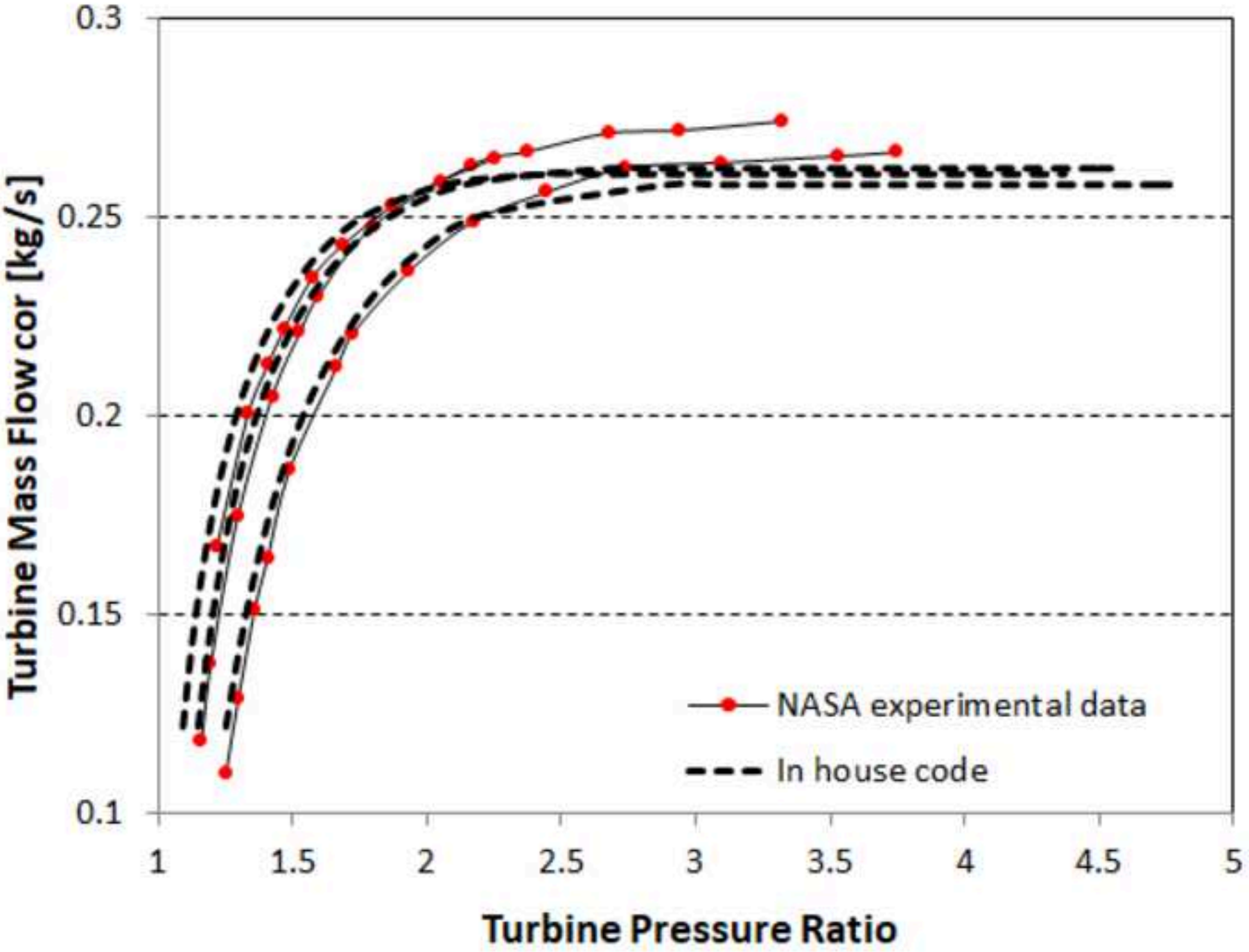


Figure 6

Click here to access/download;Figure;Fig6.tif

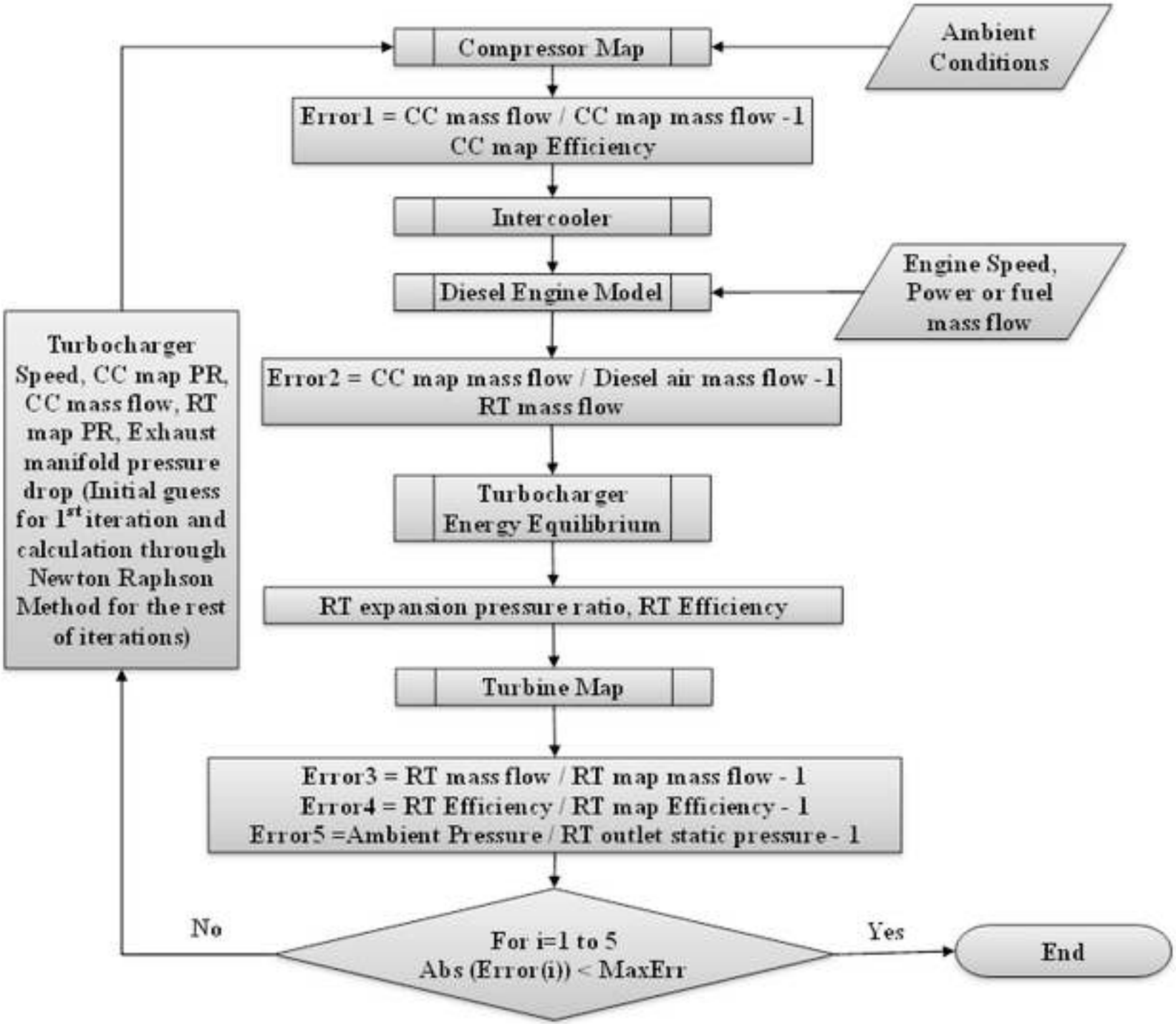


Figure 7

Click here to access/download;Figure;Fig7.tif

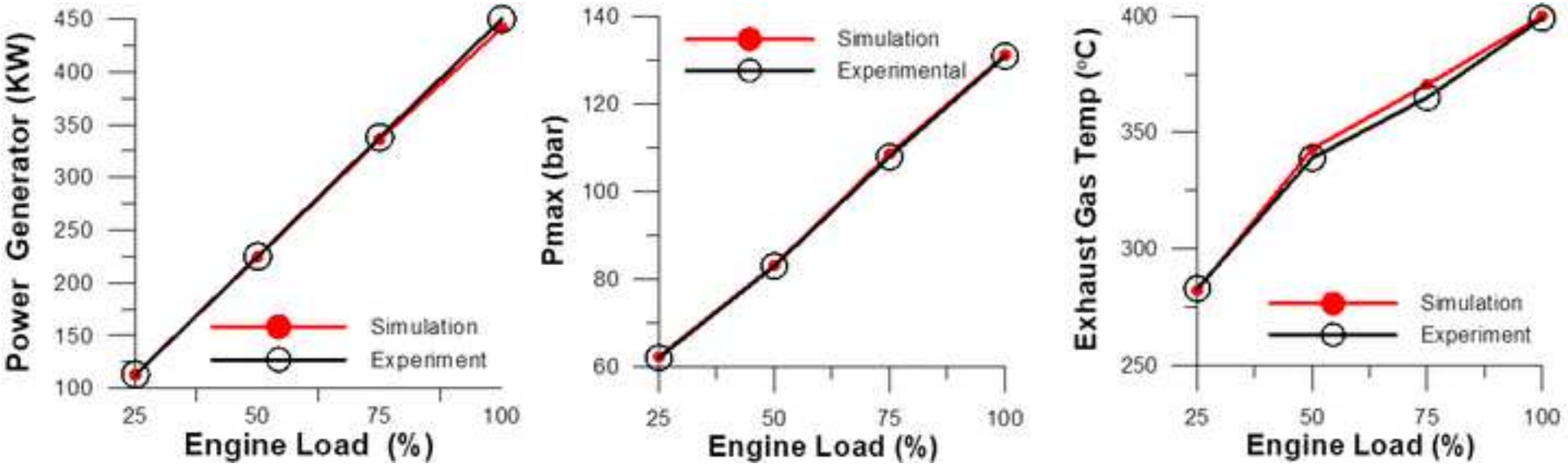


Figure 8

Click here to access/download;Figure;Fig8.tif

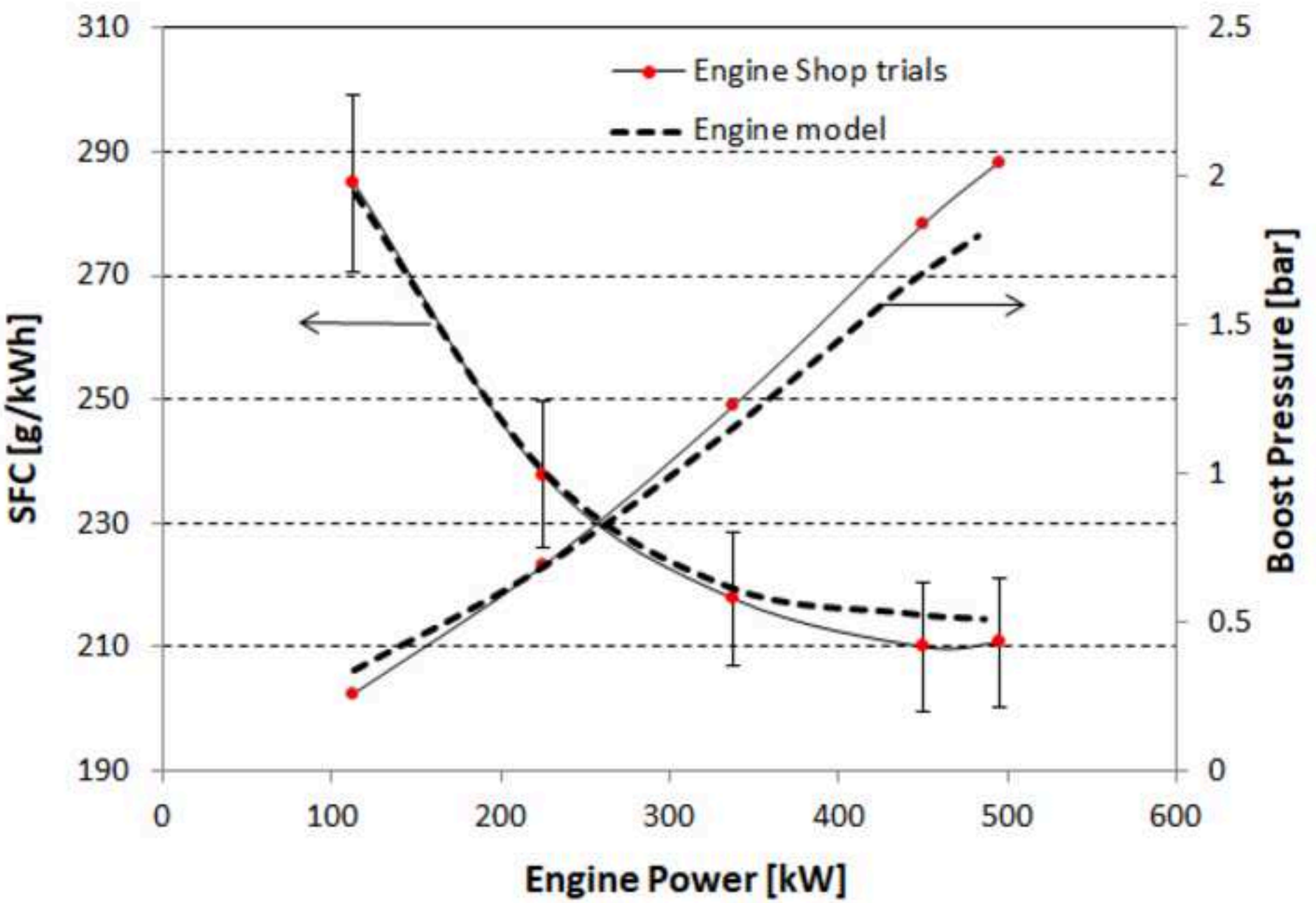


Figure 9

Click here to access/download;Figure;Fig9.tif

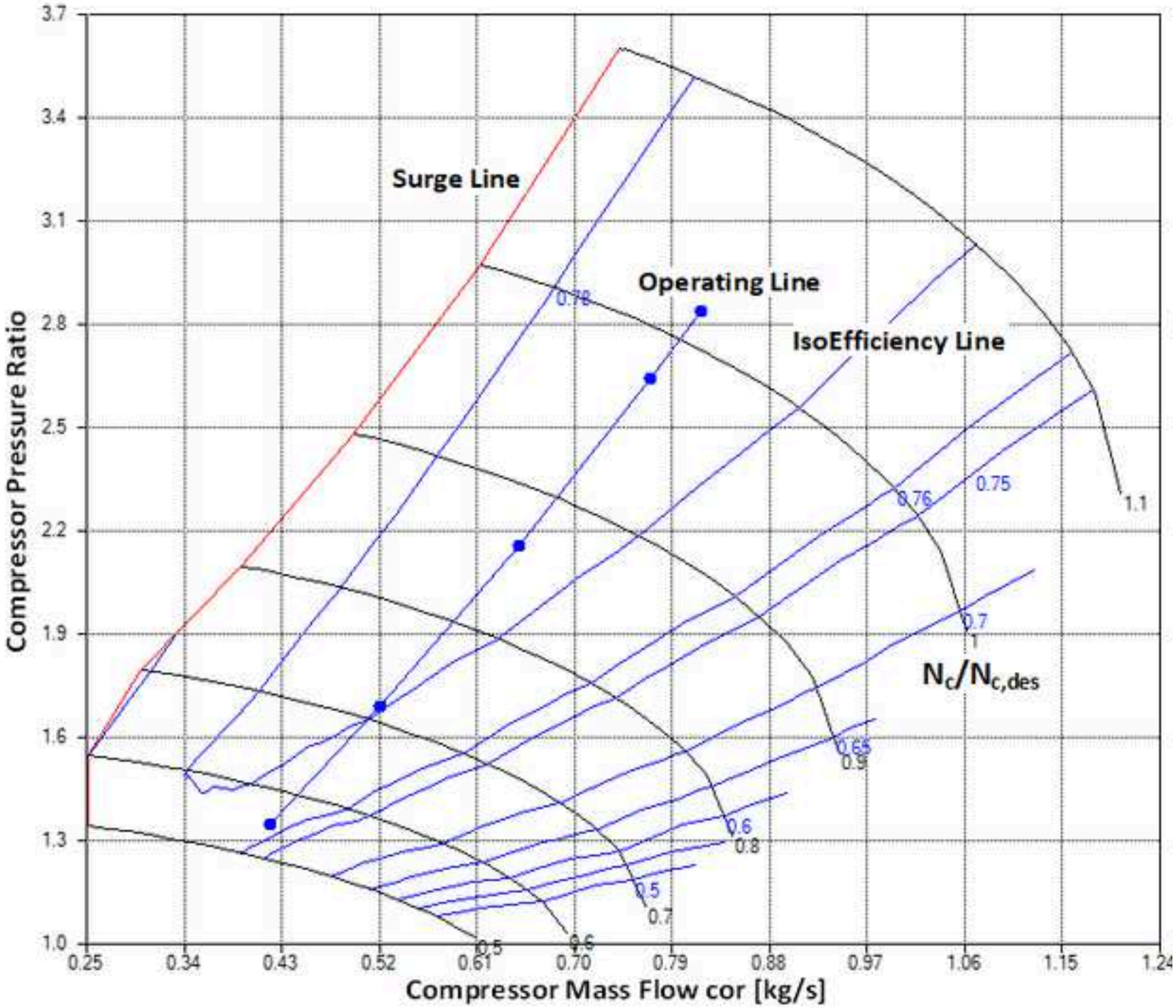


Figure 10

Click here to access/download;Figure;Fig10.tif

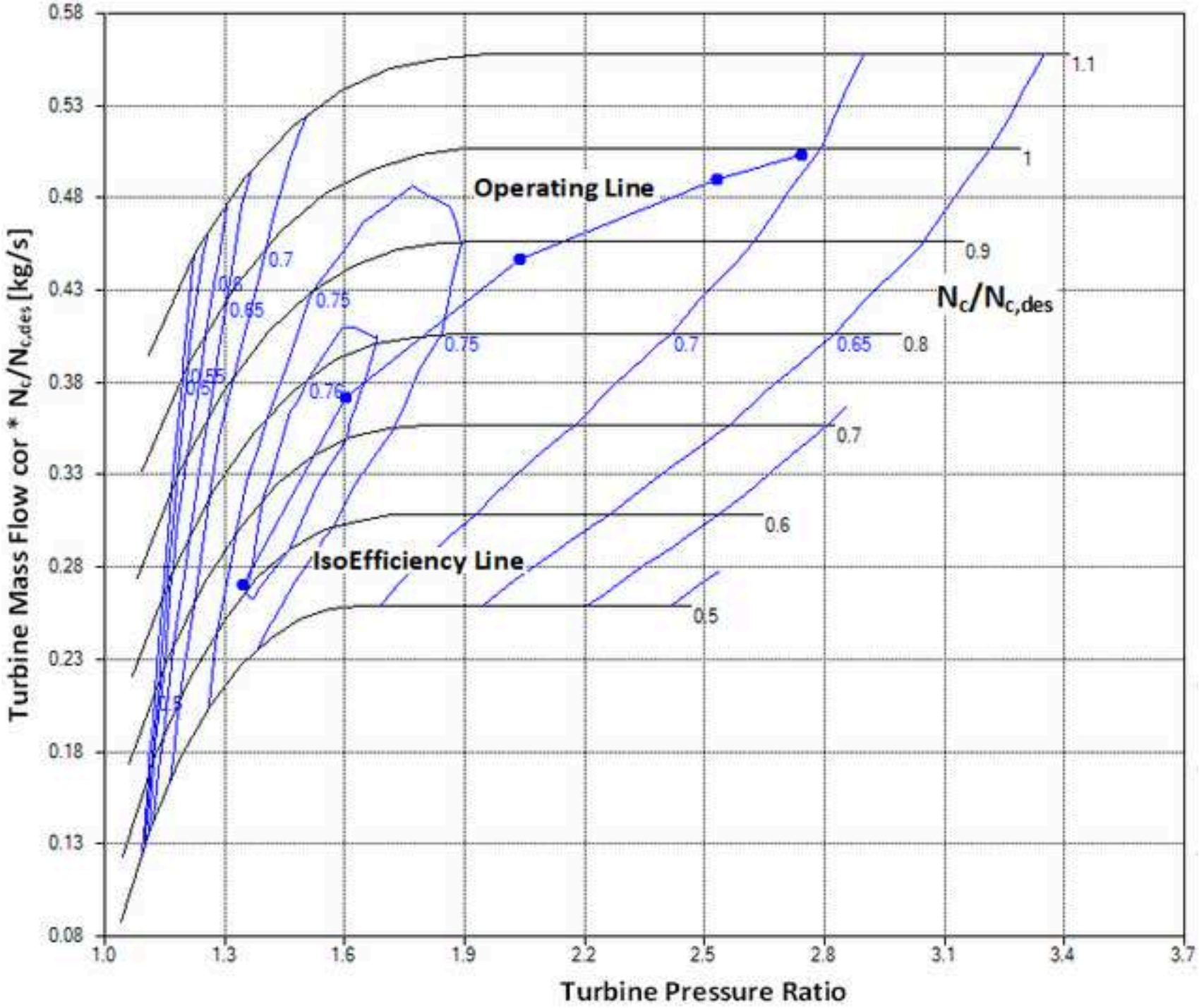


Figure 11

Click here to access/download;Figure;Fig11.tif

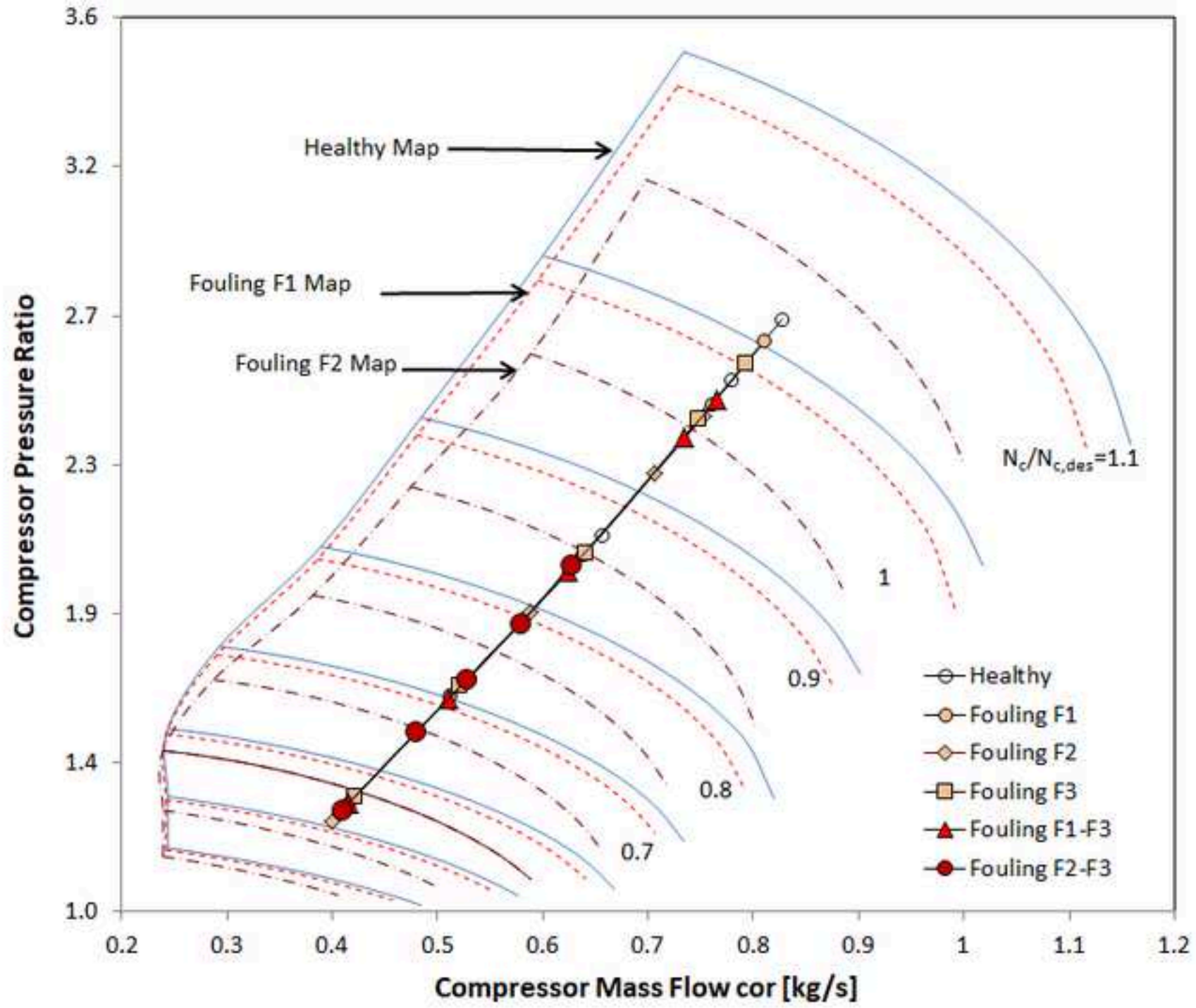


Figure 12

Click here to access/download;Figure;Fig12.tif

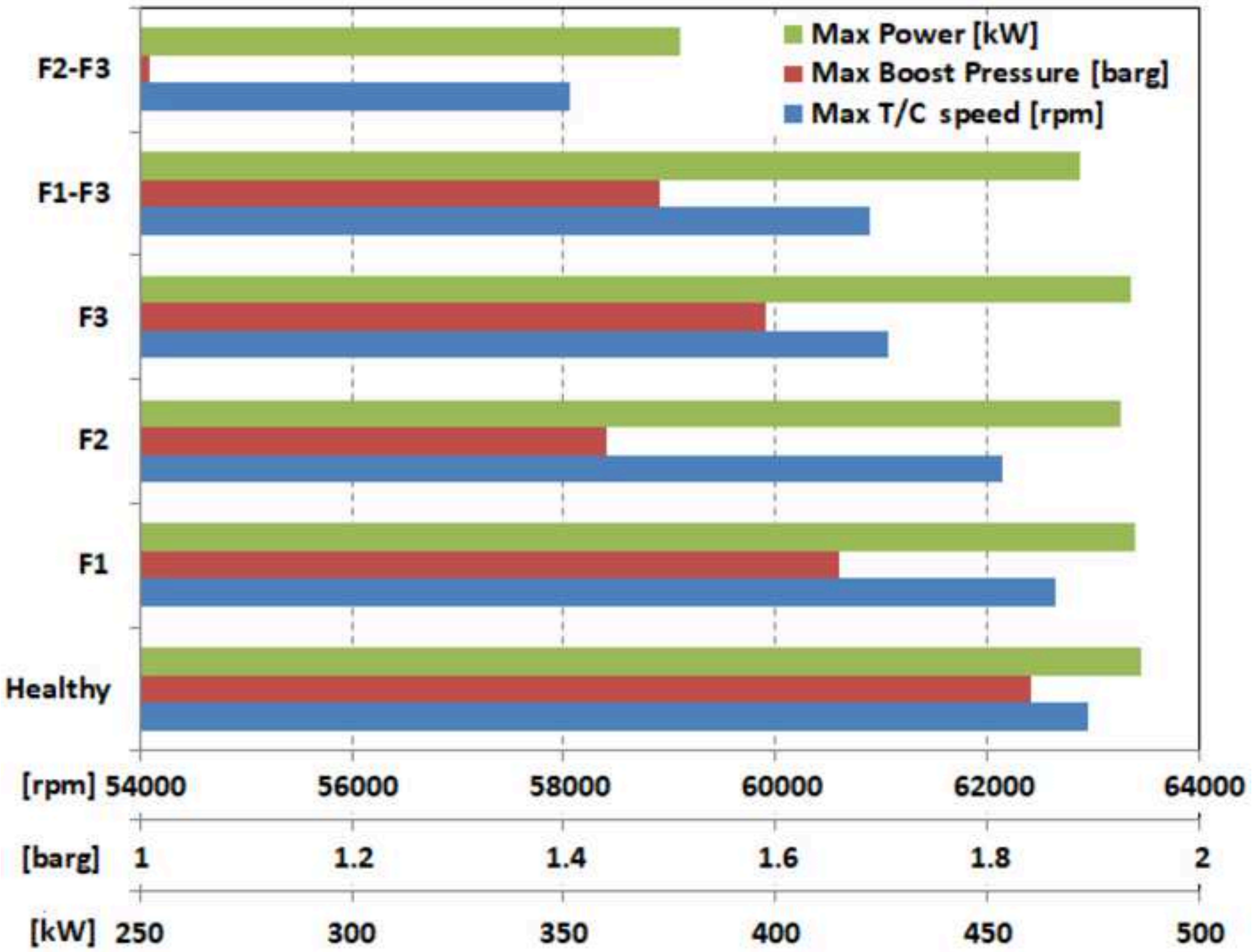


Figure 13

Click here to access/download;Figure;Fig13.tif

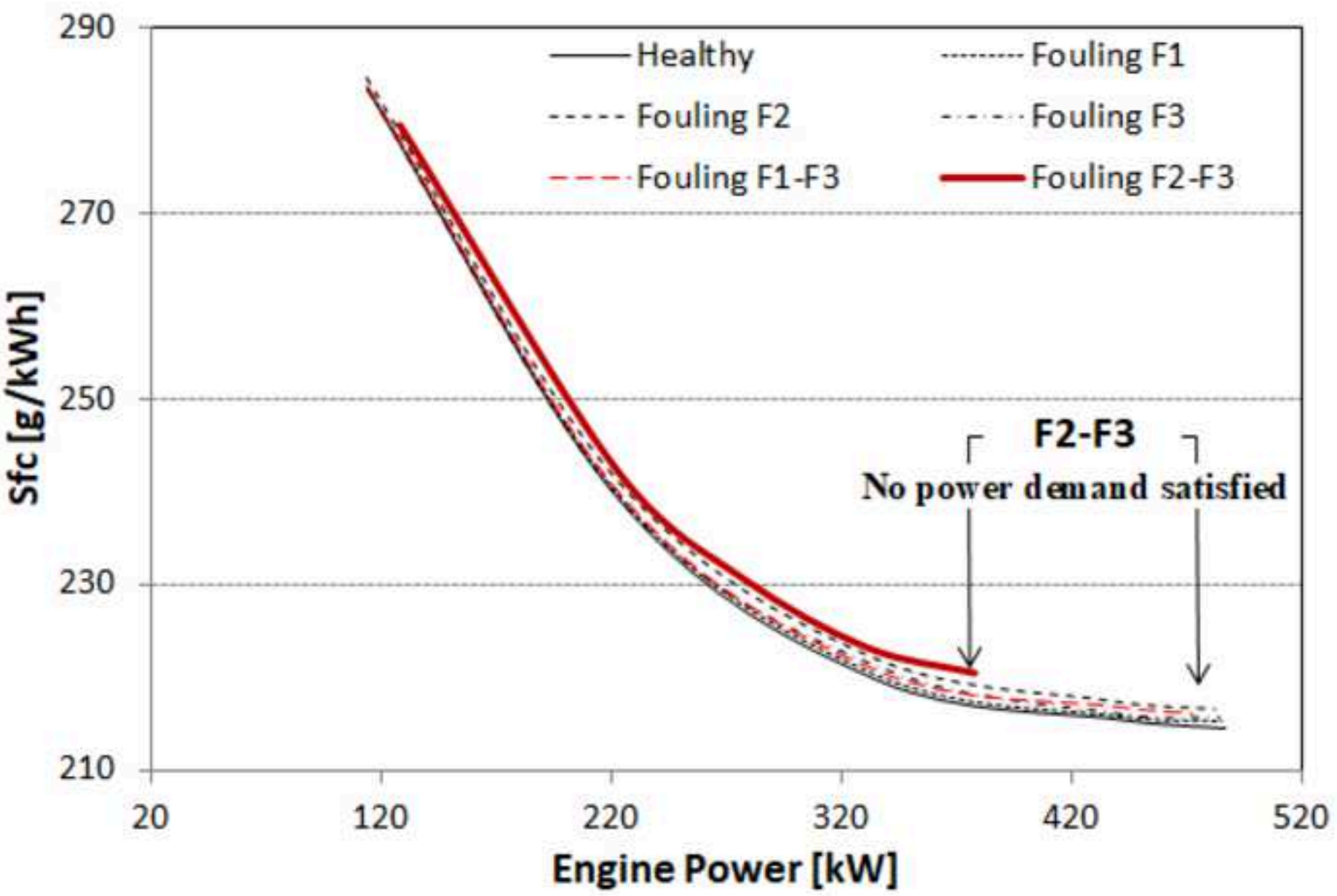


Figure 14

Click here to access/download;Figure;Fig14.tif

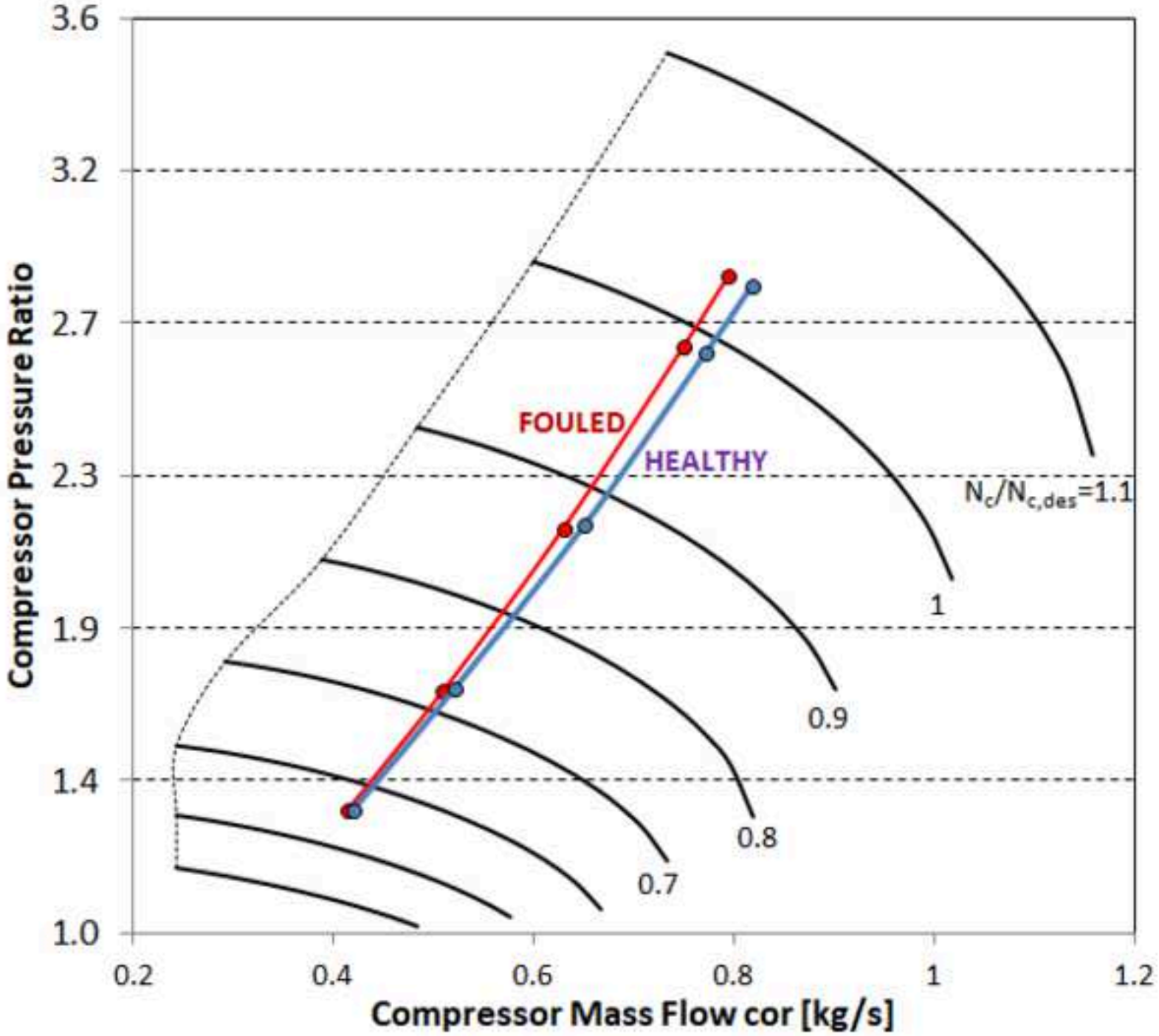


Figure 15

Click here to access/download;Figure;Fig15.tif

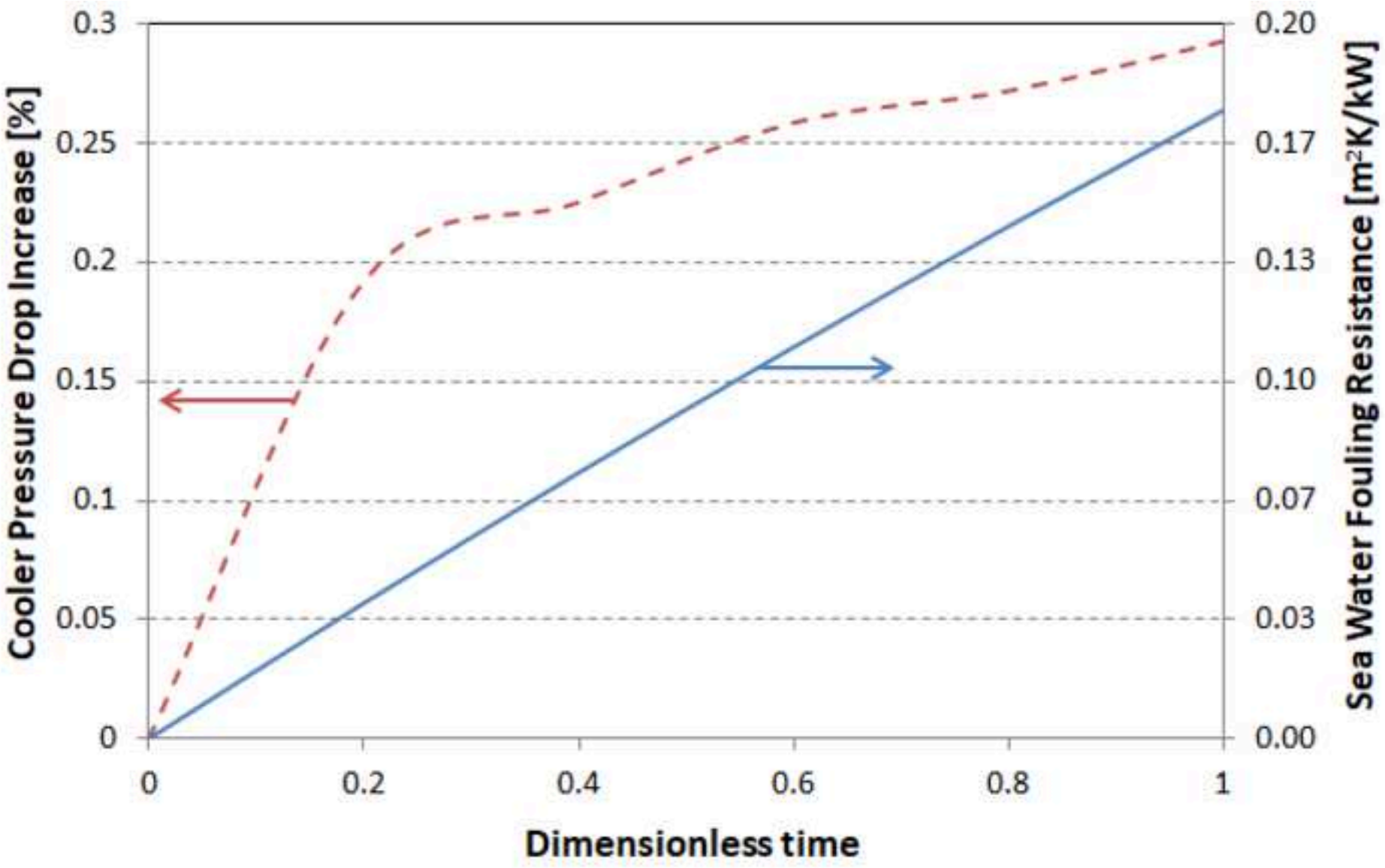
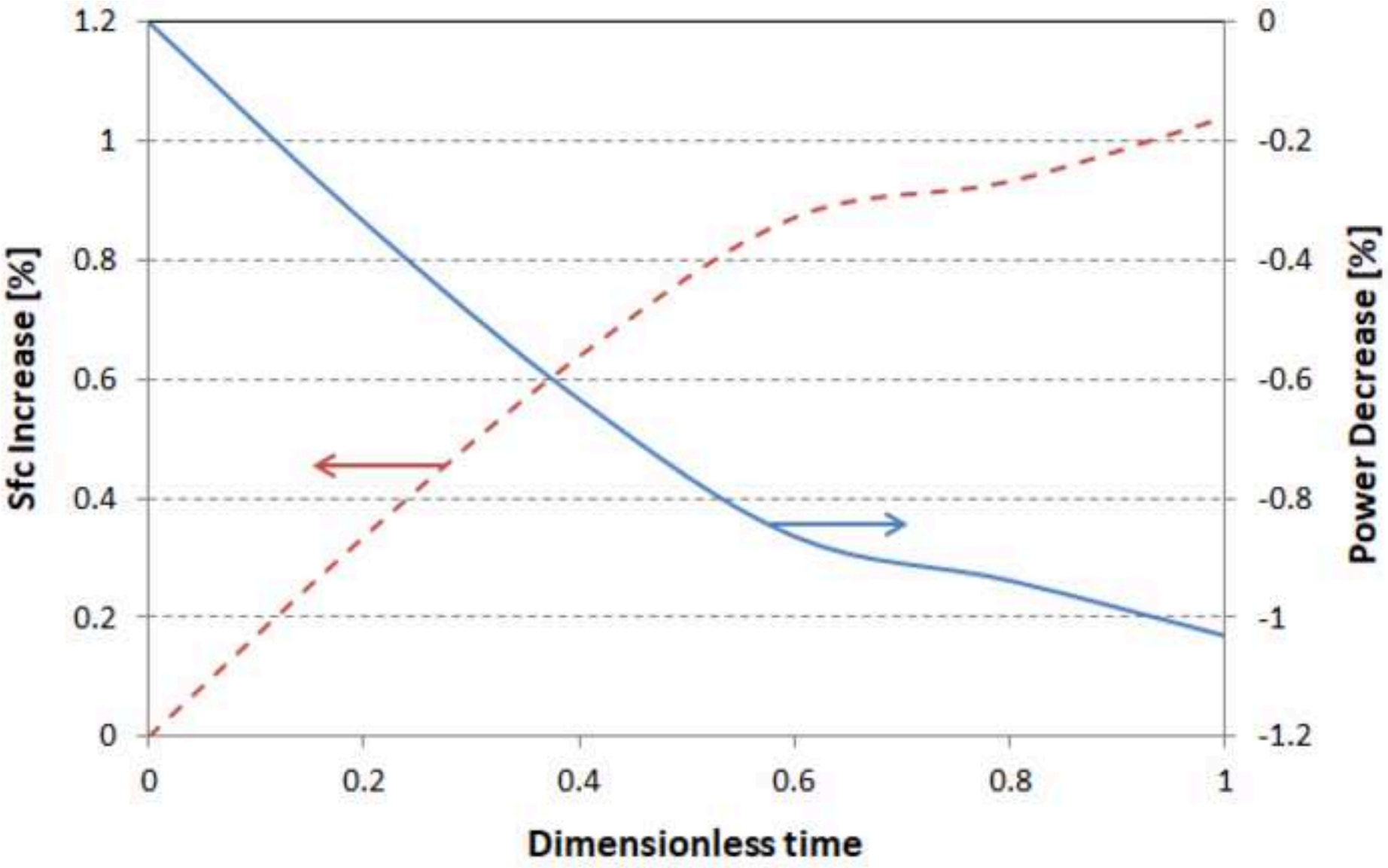


Figure 16

Click here to access/download;Figure;Fig16.tif



List of Figures

1. Fig. 1. Centrifugal compressor geometry specifications
2. Fig. 2. In house CC code validation with NASA experimental data (total pressure ratio)
3. Fig. 3. In house CC code validation with NASA experimental data (efficiency)
4. Fig. 4. Radial turbine geometry specifications.
5. Fig. 5. In house RT code validation with NASA experimental data
6. Fig. 6. Coupling between T/C and diesel engine model
7. Fig. 7. Comparison between calculated and measured values used for model calibration.
8. Fig. 8. Comparison between calculated and measured Sfc and boost pressure
9. Fig. 9. Healthy compressor map and operating line
10. Fig. 10. Healthy turbine map and operating line
11. Fig. 11. Compressor map and operating line change due to fouling
12. Fig. 12. Engine power, boost pressure and T/C speed variation due to fouling
13. Fig. 13. sfc variation due to fouling
14. Fig. 14. Operating line movement due to intercooler fouling
15. Fig. 15. Intercooler fouling pressure drop and resistance against time
16. Fig. 16. Sfc and power change rate due to fouling



https://dspace.org/

Integrated simulation framework for assessing turbocharger fault effects on diesel-engine performance and operability

Ntonas, Konstantinos; Aretakis, Nikolaos; Roumeliotis, Ioannis; Pariotis, Efthimios; Paraskevopoulos, Yiannis ...

2020-08-01
American Society of Civil Engineers (ASCE)
https://doi.org/10.1061/(ASCE)EY.1943-7897.0000673
Ntonas K, Aretakis N, Roumeliotis I, et al., (2020) Integrated simulation framework for assessing turbocharger fault effects on diesel-engine performance and operability. Journal of Energy Engineering, Volume 46, Issue 4, August 2020, Article number 04020023

Downloaded from a DSpace repository. https://dspace.org/